Dear Editor,

We would firstly like to thank again the three referees for the very comprehensive review of our manuscript and their extensive comments and remarks. This has helped us immensely improving the quality of the paper and we appreciate the work and time invested by the referees. In summary, the referees have made the following major comments:

- Many parts of the manuscript are too long, unstructured and imprecise
- More (recent) references should be added to the Introduction and/or Discussion sections
- No scenario with a salinity gradient calculated
- Injection of water instead of CO_2
- Varying fault permeabilities only calculated for closed reservoir boundaries
- Results are similar to the findings of Tillner et al. (2013)
- Discussion on the complexity of fault zones / how the applied fault architecture does fit in here

Based on these comments, we have completely revised most parts of the manuscript and shortened it by about four pages. We have considered all major and minor/specific comments and suggestions in our revised manuscript, as already described in detail in the Answer comments (please refer to the files AC_C3536, AC_C3543, AC_C3591 and AC_C3575). We will not list all changes in detail here and will only touch upon the major revisions. All changes made are tracked in the file hess-2015-163-manuscript-version2. In summary, we have done the following major revisions:

1) We have changed the order of authors to: E. Tillner, M. Langer, T. Kempka and M. Kühn

2) TITLE: As suggested by Referee 3, we decided to change the title to:

   "Fault damage zone volume and initial salinity distribution determine intensity of shallow aquifer salinization in geological underground utilization."

3) ABSTRACT: It was remarked by the referees that this section is too unstructured, with too much information being introduced in one paragraph that make it difficult to follow even after reading the entire paper. We have shortened and rewritten the Abstract and kept the description of the paper findings general enough without referring to specific scenarios to achieve the desired clarity and precision. We revised the remarked paragraph as follows:

   "Higher vertical pressure gradients for short fault segments or a small effective fault damage zone result in the highest salinization potential due to a larger vertical fault height affected by fluid displacement. Consequently, it has a strong impact on the

degree of shallow aquifer salinization, if a gradient in salinity exists or the salt-freshwater interface lies below the fluid displacement depth in the faults. A small effective fault damage zone volume or low fault permeability further extend the duration of fluid flow, which can persist for several tens to hundreds of years, if the reservoir is confined laterally. Laterally open reservoir boundaries, large effective fault damage zone volumes and intermediate reservoirs significantly reduce vertical brine migration and the potential of freshwater salinization because the origin depth of displaced brine is located only a few decametres below the shallow aquifer in maximum."

4) Section 1 – INTRODUCTION: We have integrated more citations, as recommended. It was further remarked that the reason for the different modelling results of the study conducted by Person et al. (2010) and Zhou et al. (2010) is not described in the introduction. We revised the above mentioned comments as described below. Furthermore, we included the paper of Person et al. (2010) also in Table 1, as recommended.

"Especially fault zones are of particular importance, as they might transect several caprocks and thus can provide large-scale permeable conduits between aquifers at different depths (Dempsey et al., 2014; Fitts and Peters, 2013; Chiaramonte et al., 2008; IEAGHG, 2008; Bense and Person, 2006; Forster and Evans, 1991). (…) The disparity between the simulation results is mainly related to the fact that Person et al. (2010) assumed considerably lower reservoir formation permeability, higher formation compressibility and closed lateral flow boundaries except for the northern model domain, whereas Zhou et al. (2010) applied laterally open flow boundaries (Table 1)."

5) Section 2 – STUDY AREA: It was commented that this chapter is too long; the geology in the study area is described very detailed, while in the end a rather simple model is used. Therefore, we have shortened this section by about 50 %. Now only geological characteristics in the study area that are relevant for model implementation or parameterization are described briefly for a short overview.

6) Section 3.3 – INITIAL AND BOUNDARY CONDITIONS: The referees commented that the effect of the initial salinity distribution on the degree of shallow aquifer salinization is not tested in the paper. Therefore, we have performed two additional simulations considering a linear salinity gradient in addition to the scenarios with sharp salt-/freshwater interface and revised Section 3.3 as described below. A comparison between scenarios with salinity gradient and a sharp salt-/freshwater interface is presented in the new Results Section 5.6: Salinity gradient.

"Salinity is assumed to increase with depth either by a gradient of 0.23 g kg^{-1} solution per meter from zero at the base of the Rupelian basal sand up to a maximum of 25 % at

a depth of 1070 m (Vattenfall, 2009) or sharply from zero in the Rupelian to 25 % below that aquifer. The last conditions were chosen, as they lead to the maximum possible salinization in the uppermost aquifer, and thus represent the most unfavourable scenario for shallow aquifers under the given assumptions."

7) Section 3.3 – INITIAL AND BOUNDARY CONDITIONS: The reason why we injected brine instead of CO_2 is now described in the manuscript as follows:

"In the respective industrial project at the Beeskow storage site, it was planned to inject 34 Mt of CO_2 over a time span of 20 years into the Mesozoic formations at the top of an anticline structure (Tillner et al., 2013). In the present study, the equivalent volume of brine was injected into the storage formation instead of CO_2, which enables us to study also the long-term effects of brine displacement more than 1 000 years after the injection stop. Without topographic variations in the reservoir, CO_2 is not immobilized in structural traps (e.g. below an anticline top) and might reach the Fuerstenwalde-Guben fault zone located at a distance of 4 km from the injection well over such a long simulation period, which should not be focus of investigation in the present study. Furthermore, with such a model we keep the findings of injection-related brine displacement transferable to various other types of subsurface storage."

However, as recommended by the referees, we performed one additional simulation, in which we injected 34 Mt of CO_2 over a time span of 20 years into the storage formation, instead of the equivalent volume of brine to demonstrate potential differences in displaced brine mass. We have chosen Scenario $F_{1\text{-}4}{}^{193\ km}\ B_C$ for this comparison, with four open faults with a permeability of 700 mD, closed reservoir boundaries, no secondary reservoir above the storage formation and an initial salinity increasing sharply from 0 in the shallow aquifer (Rupelian basal sand) to 25 % below this aquifer. The simulation results presented in Figure a. and b. demonstrate that injecting brine instead of CO_2 can be well applied in salinization assessments since brine displacement is only slightly overestimated. Figure a. shows the mass of salt (red) and water (blue) that is displaced out of the injection horizon through the faults and into the uppermost formation in our model (Rupelian basal sand) after 20 years (left) and 500 (years) for both cases: injection of CO_2 and injection of brine. Due to compressibility effects of the CO_2, the amount of salt and water displaced into the shallow aquifer after 20 years is only little less when injecting CO_2 instead of brine. After a simulation time of 500 years, the difference in the relative mass change in the shallow aquifer when injecting brine is also not significant.

The pressure development at the base of Fault 1 (Figure b) is very similar when comparing both injection scenarios. The slightly lower reservoir pressure when injecting CO_2 explains slightly lower brine masses displaced into the shallow aquifer as described above.

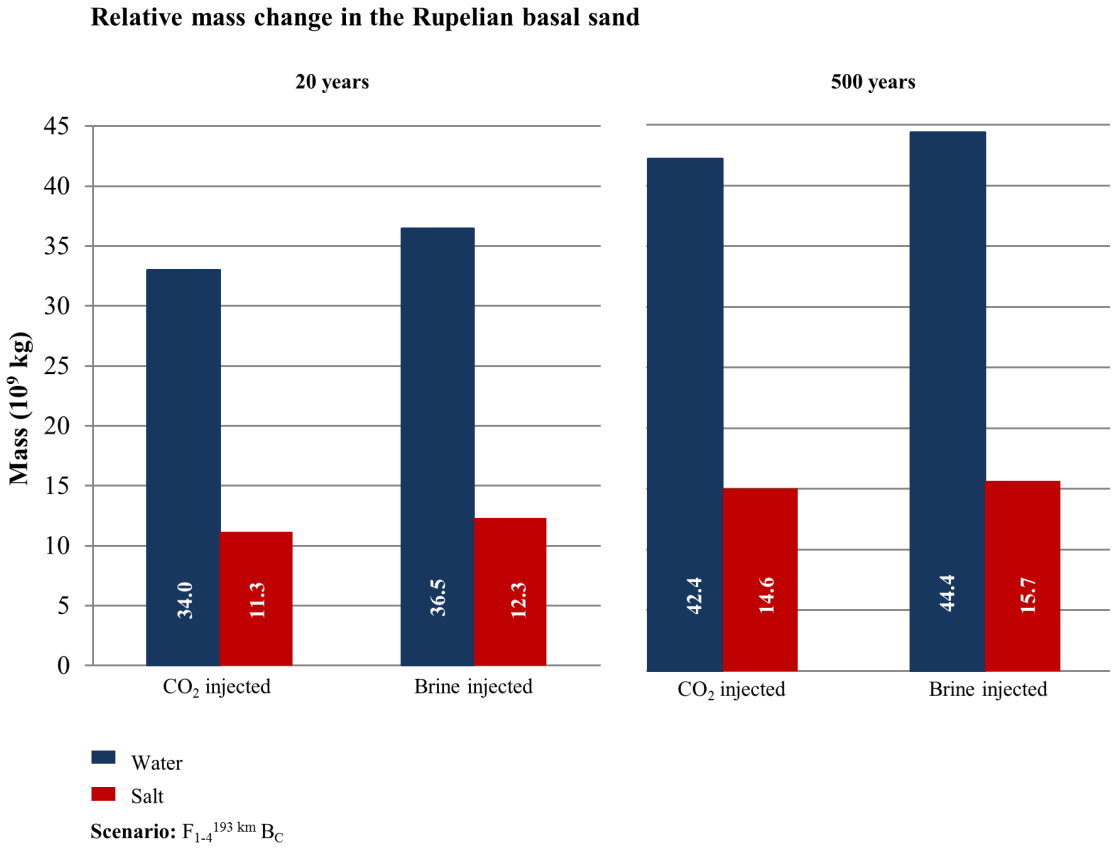

Figure a.

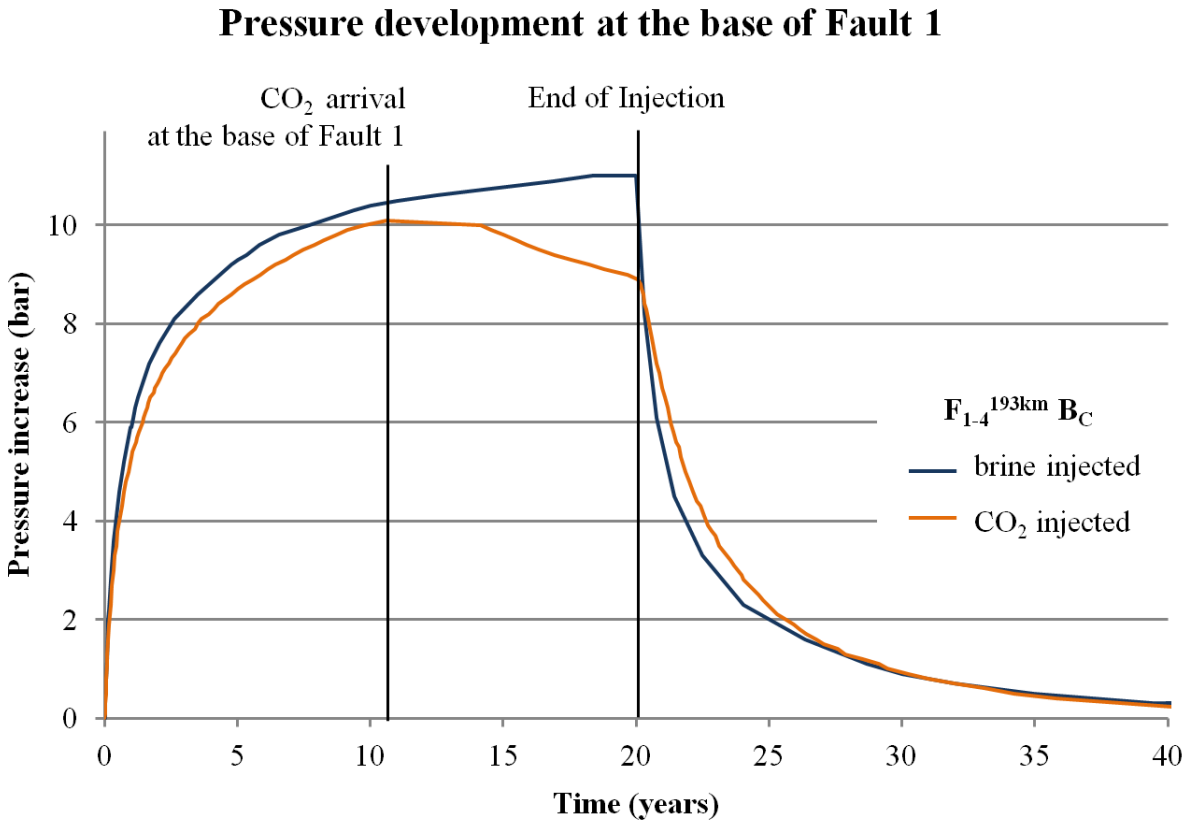

Figure b.

8) Section 4 – SET OF SCENARIOS: This section has been shortened by about 40 % as well. As recommended, the term “effective damage zone volume” is introduced earlier than in the discussion. We have added the effective damage zone volumes for the three different fault lengths to the manuscript. The fault element volume can be derived from TOUGH2, the effective porosity is known as well.

“Based on the effective porosity assumed for all fault zones and the total fault element volumes, the effective damage zone volume of the faults for the three different cases can be specified with 1.6×10^{10} m^3 (fault length of 193 km), 4.9×10^{9} m^3 (fault length of 60 km) and 1.8×10^{8} m^3 (fault length of 2 km), respectively.”

9) Section 5 – RESULTS: It was commented by the referees that this section is difficult to follow since it is not clearly structured and too long and the reader might lose the goal of the paper. Therefore, we have completely rewritten this section and subdivided it in six subsections. First, we give an overview at which time we have analysed pressures and relative mass changes in the shallow aquifer and which assumptions have been made in each subchapter. For a better comparability of the results, relative mass changes in the uppermost aquifer should not be analysed at the end of the fluid flow process, since this moment of time is not identical in all scenarios. As recommended, we have revised that and analysed brine displacement at 20 years corresponding to the end of the injection period. In the first subsection, we present general outcomes that are valid for all simulated scenarios. The impact of fault length, overlying secondary reservoir, fault permeability, permeability difference between fault and secondary reservoir and the salinity gradient on shallow aquifer salinization is then presented in the following five subsections:

5 Results

“Results of injection induced brine displacement via the faults are analysed at 20 years corresponding to the end of the injection period. At this time, reservoir pressures have reached their maximum, and thus effects on upward brine flow are most noticeable. In Sections 5.2 to 5.5, salinity is assumed to increase sharply from zero in the Rupelian basal sand to 25 % below that aquifer. In Section 5.6, the impact of a salinity gradient on shallower aquifer salinization is presented. Here, salinity in the fault(s) increases from zero at the base of the Rupelian up to a maximum of 25 % at a depth of 1 070 m. Fault permeability is 700 mD in all investigated scenarios, except for the comparison presented in Section 5.4, where duration of mass flow and shallow aquifer salinization are investigated also for lower fault permeabilities of 10 mD and 200 mD. In Section 5.5, it is shown how a secondary reservoir with a permeability higher than that of the faults affects upward brine migration.

5.1 General outcomes
5.2 Fault length / effective damage zone volume
5.3 Overlying secondary reservoir
5.4 Fault permeability
5.5 Permeability difference between fault and secondary reservoir
5.6 Salinity gradient

(…)."

In order to make the results more easily understandable to the reader, we have completely revised Table 3 and integrated an additional Table 4. In both tables, all calculated scenarios are listed starting with the scenario with the highest relative salt mass change in the shallow aquifer to the lowest. As recommended by the referees, we have replaced the lateral distance in the shallow aquifer that is affected by salinization by the total area. The mass of brine displaced into the shallow aquifer is for instance almost identical when comparing the scenario with a sharp salt-/freshwater interface with the corresponding scenario with a salinity gradient. However, salt concentrations are significantly lower if a salinity gradient was applied. Therefore, salinization of the shallow aquifer is now indicated in text and tables and figures by relative salt mass changes or the average salt mass in the area affected by salinization for each scenario rather than the displaced mass of brine. The referees further commented that we demonstrated the effect of different fault permeabilites only for laterally closed reservoir boundaries. Therefore, we have conducted three additional scenarios with three different fault permeabilities and open reservoir boundaries. The results are presented in Section 5.4. In this context, also Figure 3 was revised.

10) Section 6 – DISCUSSION: We have completely rewritten the Discussion Section. We discussed our results with more recent publications and integrated recommended literature. We further included a discussion on the complexity of fault zones and explained for which fault architecture the results presented in our study are valid. The main differences to the findings of Tillner et al. (2013) have been made clearer now in the discussion.

11) REFERENCES: The reference list was completely revised. We integrated all additional references and corrected minor mistakes in the citation format.

12) TABLES/FIGURES: Table 1 has been revised (we included the paper of Person et al., 2010, as recommended). Table 3 has been completely revised. We integrated a new Table 4, in which we compare the scenarios with different fault permeabilities. We revised most of the Figures (order has been changed) and integrated a new Figure 14 that illustrates the difference in the relative salt and water mass changes in the shallow aquifer, if a sharp salt-/freshwater interface or a salinity gradient is assumed.

On behalf of all co-authors, many thanks and best regards
Elena Tillner

~~Effective~~Fault damage zone volume ~~of fault zones~~ and initial salinity distribution determine intensity of shallow aquifer salinization in geological underground utilization

~~M. Langer[1],~~ E. Tillner[1], M. Langer[1], T. Kempka[1] and M. Kühn[1,2]

[1]{GFZ German Research Centre for Geosciences~~, Section 5.3 Hydrogeology~~, Telegrafenberg, 14473 Potsdam, Germany}

[2]{University of Potsdam, Institute of Earth- and Environmental Science, ~~Am Neuen Palais 10, 14469~~Karl-Liebknecht-Str. 24/25, 14476 Potsdam, Germany}

Correspondence to: E. Tillner (elena.tillner@gfz-potsdam.de)

Abstract

Injection of fluids into deep saline aquifers causes a pore pressure increase in the storage formation, and thus displacement of resident brines. Via hydraulically conductive faults, brine may migrate upwards into shallower aquifers, and lead to unwanted salinization of potable groundwater resources. In the present study, we investigated different scenarios for a ~~prospective~~potential storage site ~~close to the city of Beeskow~~ in the Northeast German Basin ~~by~~ using a 3D regional scale model ~~(100 km × 100 km × 1.34 km)~~ that includes four ~~ambient~~major fault zones. The focus was on assessing the impact of fault length and the effect of ~~an overlying~~a secondary reservoir above the storage formation, as well as model boundary conditions and initial salinity distribution on the potential salinization of shallow groundwater resources. We employed numerical simulations of brine injection as a representative fluid using the simulator TOUGH2-MP.

Our simulation results demonstrate that the lateral model boundary settings and the effective fault damage zone volume have the greatest influence on pressure build-up and development within the reservoir~~ determines the~~, and thus intensity and duration of fluid flow through the faults~~, and hence~~. Higher vertical pressure gradients for short fault segments or a small effective fault damage zone result in the highest salinization ~~of shallower aquifers. Application of different boundary conditions proved that these have a crucial~~potential due to a

larger vertical fault height affected by fluid displacement. Consequently, it has a strong impact on the degree of shallow aquifer salinization, if a gradient in salinity exists or the salt-freshwater interface lies below the fluid displacement depth in the faults. A small effective fault damage zone volume or low fault permeability further extend the duration of fluid flow, which can persist for several tens to hundreds of years, if the reservoir ~~fluid displacement. If~~is confined laterally. Laterally open reservoir boundaries ~~are closed, the fluid migrated upwards into the shallow aquifer, corresponds to the overall injected fluid mass. In that case, a short hydraulically conductive fault length and the presence of an overlying secondary reservoir leads only to retardation in~~ , large effective fault damage zone volumes and intermediate reservoirs significantly reduce vertical brine ~~displacement up to a factor~~migration and the potential of ~~five and three, respectively. If the reservoir boundaries are open, salinization is considerably reduced: In the presence~~freshwater salinization because the origin depth of ~~a secondary reservoir, 33 % of equivalent~~ displaced brine ~~mass migrates into~~is located only a few decametres below the shallow aquifer~~, if all four faults are hydraulically open over their entire length, whereas the displaced equivalent brine mass is only 12 % for a single fault of two kilometres length. Taking into account the considered geological boundary conditions, the brine originates~~ in maximum ~~from the upper 4 m to 298 m of the investigated faults. Hence, the initial salt-freshwater interface present in the fault is of high relevance for the resulting shallow aquifer salinization.~~ .

The present study demonstrates that the existence of hydraulically conductive faults is not necessarily an exclusion criterion for potential injection sites, because salinization of shallower aquifers strongly depends on initial salinity distribution, location of hydraulically conductive faults and their ~~length~~effective damage zone volume as well as geological boundary conditions. ~~These constraints are location specific, and need to be explored thoroughly in advance of any field activity. They provide the basis for scenario analyses and a reliable risk assessment.~~

1 Introduction

Carbon Capture and Storage (CCS) can contribute to the reduction of global anthropogenic carbon dioxide emissions. Different geological underground formations have been suggested as target storage sites, ~~whereby~~such as deep saltwater-bearing aquifers (saline aquifers ~~provide~~) providing the worldwide largest storage potential as part of the earth's widely

Formatted: English (U.S.)

distributed sedimentary basins (IPCC, 2005). ~~Due to their extent and storage capacity, shallow~~Shallow aquifers in sedimentary basins can comprise ~~also~~ considerable freshwater resources, which in turn are of great importance for regional water supply. However, brine displacement due to the elevated pore pressure in the storage formation is one potential risk of CO_2 storage in deep saline aquifers. Saline fluids could reach shallower freshwater aquifers through different migration pathways, and significantly impair groundwater quality. Especially fault zones are of particular importance, as they ~~form potential weakness zones within the host rock, and~~ might ~~act as~~transect several caprocks and thus can provide large-scale permeable conduits ~~penetrating several caprocks.~~between aquifers at different depths (Dempsey et al., 2014; Fitts and Peters, 2013; Chiaramonte et al., 2008; IEAGHG, 2008; Bense and Person, 2006; Forster and Evans, 1991).

Displacement of brine and potential freshwater salinization as a result of CO_2 storage has been investigated in several studies. Table 1 summarizes the initial conditions and essential results of numerical simulations concerning this issue. The models applied are either synthetic (Birkholzer et al., 2011; Oldenburg and Rinaldi, ~~2011; Birkholzer et al.,~~ 2011; Birkholzer et al., 2009) or refer to a certain study area (Tillner et al., 2013; Zouh et al., 2010; Yamamoto et al., 2009; Nicot ~~et al.,~~ 2008). Several studies examine pressure perturbation and resulting brine migration in a multi-barrier system without considering vertical conduits. It was shown that pressure build-up can be observed in a distance of more than 100 km from the injection zone (Birkholzer et al., 2009). ~~Thereby, the~~The choice of ~~initial~~boundary conditions and petrophysical parameters have a crucial impact on the pressure development, as demonstrated by two independent studies considering industrial-scale CO_2 injection in the Illinois Basin (Person et al., 2010; Zhou et al., 2010). After Person et al. (2010), the pressure perturbation is limited to a distance of about 25 km from the injection location for a total injection rate of 80 Mt CO_2 $year^{-1}$, whereas Zhou et al. (2010) simulated a pressure build-up as far as 300 km from the injection area (100 Mt CO_2 $year^{-1}$). The disparity between the simulation results is mainly related to the fact that Person et al. (2010) assumed considerably lower reservoir formation permeability, higher formation compressibility and closed lateral flow boundaries except for the northern model domain, whereas Zhou et al. (2010) applied laterally open flow boundaries (Table 1).

However, upward brine migration only occurs if pressure perturbation in the reservoir is large enough to overcome the weight of the fluid column in a vertical conduit. ~~It~~ If a steady-state is

Formatted: Font color: Black, English (U.S.)

Formatted: Font color: Black, English (U.S.)

Formatted: English (U.S.)

reached or continuous flow develops further depends on the magnitude of pressure increase, and whether brine is allowed to spread ~~laterally~~unhindered in the upper aquifer~~, if~~ due to a ~~steady state is reached or~~ continuous hydraulic connection throughout the formation without barriers to flow ~~develops ((~~Birkholzer et al., 2011; Oldenburg und Rinaldi, 2011~~; Birkholzer et al., 2011~~). ~~Especially~~As stated previously, especially faults can represent vertical conduits, which may have an essential influence on groundwater flow and brine migration due to their extent and distribution in the Earth's upper crust. Nevertheless, a meaningful implementation of complex geological structures into a sufficiently discretised model grid is very difficult, especially at regional scale. Tillner et al. (2013) investigated the influence of permeable faults on brine displacement referring to a real study area. The authors simulated upward brine migration through complex fault systems depending on reservoir compartmentalisation and fault permeability, whereby faults were implemented by the virtual element approach (Nakaten et al., 2013). The results of Tillner et al. (2013) ~~indicates~~show that the degree of pressurization is the driving mechanism for brine migration, while an increase of fault permeability ~~of fault zones does not influence~~from 100 mD by two orders of magnitude had no significant impact on the salinization of shallower aquifers ~~significantly~~. Their investigations focused on the prospective storage site Beeskow-Birkholz (in the following only referred to as Beeskow) in Northeast Germany, which is also considered in this work.

Here, we present a regional scale 3D model with a simplified geometry, neglecting topographic variations of the formation tops and bases while the four considered fault zones are implemented with their complex arrangement and curvature~~. Hence, the~~ to focus the analysis on clearly identifiable effects of fault fluid flow. The presumed simplifications ~~should avoid~~further significantly improved the convergence efficiency of the simulations and avoided numerical artefacts~~, and serve for improved comprehensibility of the relevant processes.~~. In different leakage scenarios the ~~effect~~impact of fault lengths, hydrogeological boundary conditions, initial salinity distribution and the presence of an overlying secondary reservoir on upward brine displacement ~~as a result of fluid injection~~ were assessed~~. The goal of this study was~~ to deepen ~~the general~~our understanding ~~of the underlying processes, as well as to characterize the impact of all investigated parameters to obtain site specific findings~~ on potential freshwater salinization~~.~~ resulting from geological CO_2 storage in deep saline formations.

Formatted: English (U.K.)

Formatted: English (U.S.)

Formatted: English (U.S.)

2 Study area

The ~~prospective~~potential CO_2 storage site is located ~~80 km southeast of Berlin~~close to the town Beeskow in the Northeast German Basin (NEGB~~), which is part of the Southern Permian Basin (~~; Fig. 1a). ~~According~~In a respective industrial project and according to the estimated storage capacity, it was planned to inject 34 Mt CO_2 over a period of 20 years (1.7 Mt CO_2 $year^{-1}$) into ~~a Mesozoic anticline structure at Beeskow (Vattenfall, 2009). Several sandstone formations of the Middle Buntsandstein, such as the Volpriehausen, Detfurth, and Hardegsen formations form potential reservoir rocks (Fig. ~~the basal sandstones of the Detfurth Formation from the Middle Buntsandstein (Lower Triassic); (Vattenfall, 2009, 2010).~~2a).~~ ~~They consist of basal sandstones and an alternating sequence of mudstones with sandy and silty layers (Vattenfall, 2010). The Detfurth Formation is characterized by the highest effective thickness of 23 m, and was therefore chosen as target storage horizon for CO_2 injection.~~ Porous and fractured sediments of the lower Muschelkalk (Middle Triassic) represent a secondary suitable reservoir above the target storage horizon (Fig. 2a).~~.~~ A multi-barrier system of different ~~cap-rocks~~caprocks, mainly anhydrites, halites and claystones from the Upper Buntsandstein, the Middle and Upper Muschelkalk, as well as the Lower Keuper seals the Detfurth Formation and the overlying secondary reservoirs. ~~The Rupelian clay (Oligocene, Upper Tertiary) forms a regional barrier between freshwater bearing glacial sediments (Upper Tertiary and Quaternary) and the underlying saline aquifers. It is located at a depth between 150 m and 200 m (Stackebrandt, 2010). Basal sandstones of the Rupelian with a thickness varying between 2.5 m and 30 m are widespread, and mark the beginning of saltwater bearing aquifers (Grube et al., 2010). During the latest three Pleistocene glacial phases, advances of the Scandinavian ice sheets locally formed deep reaching erosion channels within the Rupelian clay. Hence, a hydraulic connection between deep saline aquifers and freshwater bearing sediments exists in some parts of the area. Depending on the pressure potential, saline water could rise and mix with potable groundwater resources. As shown by Kempka et al. (2015), salt concentrations in the Quaternary deposits and fillings of the erosion channels can locally be larger than 10 g/kg.~~The basal sandstones of the Rupelian (Oligocene, Upper Tertiary) at a depth between 100 m and 150 m in average mark the beginning of saltwater-bearing aquifers in the area (Grube et al., 2000; Stackebrandt, 1998).

The fault system of the study area consists of four regional fault zones comprising several individual faults. It divides the sedimentary cover of the study area into a regional block

structure (Mittenwalde Block; Fig. 1b). The Lausitzer Abbruch and the Fuerstenwalde-Guben fault zones with NW-SE orientation, as well as the Tauer and the Potsdam fault zones striking NE-SW, enclose this compartment. All faults are normal faults with a steep inclination (between 67.8° and 74.3° in average). ~~However, the~~The Fuerstenwalde-Guben fault zone ~~consists of several individual faults also characterized by reverse components of dip-slip. It~~ has a total length of 120 km, and is characterized by an offset of a few hundred metres ~~(Hotzan und Voss, 2013). The~~ , whereas the Lausitzer Abbruch fault zone ~~dips NE, and~~ shows displacements up to 1 000 m (Hotzan and Voss, 2013; Beutler and Stackebrandt, 2012~~). This complex system was formed during the Variscan orogeny, whereby many faults were reactivated during the Alpine orogeny (~~; Stackebrandt~~, 2010).~~ and Manhenke, 2004).

Formatted: English (U.S.)

Formatted: English (U.S.)

3 Geological model

We used the Petrel software package (Schlumberger, 2011) for the 3D geological model construction and the subsequent gridding process, and the reservoir simulator TOUGH2-MP/ECO2N for 3D multi-component flow simulations (Pruess, 2005; Zhang et al., 2008). All simulations were conducted on a high performance computing system with 256 cores. Finally, results were imported back into Petrel for visualization purposes.

3.1 Setup

The ~~implementation of the~~ 3D geological model ~~refers to the structural and geological characteristics of the study area as described above. It~~ has a horizontal extent of 100 km × 100 km and a vertical thickness of 1 340 m. ~~Figure 2b shows the geological model with a regular lateral grid resolution of 250 m × 250 m. The vertical discretisation depends on the different model layers, and ranges between 10 m and 19.9 m (Table 2). The model~~It consists of up to three layers: the Rupelian basal ~~sands~~sand as the uppermost shallow aquifer, the Muschelkalk Formation as an overlying secondary reservoir and the Detfurth Formation as lowermost reservoir~~.~~ (Fig. 2b). The Rupelian basal ~~sands are~~sand is 20 m thick and located at a depth of 110 m (Grube et al., ~~2010~~2000). The Lower Muschelkalk Formation is at 1 025 m depth and has a thickness of 140 m, while the reservoir is at 1 425 m depth with a thickness of 23 m (Tillner et al., 2013). ~~The~~ Figure 2b shows the geological model ~~is limited to the saline groundwater complex up to~~with a regular lateral grid resolution of 250 m × 250 m. The vertical discretisation depends on the ~~Rupelian clay (situated above the Rupelian basal sands~~

~~and not considered in the present~~different model~~) as regional seal~~ layers, and ranges between ~~salt~~10 m and ~~freshwater.~~19.9 m (Table 2).

In a previous study, Kühn ~~et al. (2011~~and Kempka (2015) investigated the influence of caprock permeabilities on shallower aquifer salinization at the prospective storage site Beeskow. Their results showed that for caprock permeabilities equal or lower than 10^{-17} m^2 no increase in salt concentration in formations above the reservoir has to be expected. ~~In~~ The top formation seal in the ~~present~~ study~~, we assumed that the caprocks have lower permeabilities~~ area mainly consists of marine evaporates such as anhydrite and halite with a total thickness of up to 180 m. We therefore defined ~~them~~the caprocks as impermeable for fluid flow in all simulations~~, so that~~. Thus, only the faults provide a hydraulic connection between the shallow aquifer and the reservoir. ~~Thus~~Thereto, the elements of the faults as well as the different reservoir layers were "active" in ~~our~~the simulations, whereby the elements representing the caprocks were not considered. ~~Depending on the different scenarios performed (varying fault length; with or without overlying secondary reservoir), the model consists of 635 508 to 1 811 473 active elements.~~

Within our model only the inner faults, which enclose the Mittenwalde Block were implemented as a representation of the entire fault zone (Fig. 1b). ~~Thereby~~Thereto, fault related parameters were assigned to the elements located at the respective vertical fault plane. The fault element width of 250 m corresponds to the overall lateral grid resolution. This element width is relatively large but still realistic, since all regional fault zones consist of several individual faults and show considerable displacements~~.~~ between a few hundred meter to 1 000 m. In general, fault offset is linked to the width of the damage zone (~~Wibberley et al., 2008;~~ Faulkner et al. 2010; Mitchel and Faulkner, 2009~~;~~ Wibberley et al., 2008). For example, faults with displacements between 10 m and 1 000 m can have damage zone widths between tens and hundreds of metres. However, there exists no simple relationship, since the width of the damage zone is highly dependent on lithology, pressure, temperature, and strain rate during shear and potentially tensile deformation (Shipton et al., 2006). Due to the relatively steep inclination of all faults and to maintain maximum grid regularity, the dip angle was neglected in the present model and all faults were assumed to be strictly vertical. In the following, the Fuerstenwalde-Guben fault zone is addressed as Fault 1. The Potsdam, the Lausitzer Abbruch and the Tauer fault zones are referred to as Faults 2, 3 and 4, respectively (Fig. 1b).

~~The applied geological model was considered in the numerical simulations by simplifying the original topography of the formation tops and bases to focus the analysis on clearly identifiable effects of fault fluid flow.~~

3.2 Parameterization

All lithological units were parameterized according to Tillner et al. (2013) and Vattenfall (2009), with values derived from borehole data and literature and modelled as homogenous and isotropic. The Detfurth Formation has a permeability of 400 mD, while the overlying secondary reservoir (Muschelkalk Formation) is characterized by a permeability of 200 mD (Table 2). Porosity and permeability of the Rupelian basal ~~sands were~~sand was chosen according to Tesch et al. (1987). Fault permeability was assumed higher than that of the host rock, because of fault-parallel permeability enhancement of the damage zone due to the presence of a fracture network (~~Caine et al., 1996; ~~Jourde et al., 2002~~). Thus,~~; Caine et al., 1996). A lateral barrier to groundwater flow due to a low permeable fault core was not directly considered in the simulations. However, as a conservative approach we assume that hydraulic properties of the ~~faults were chosen to be~~fault damage zones are in between ~~of~~ those of the Rupelian basal sands and the Detfurth Formation to ~~allow for analysis~~promote upward brine displacement instead of ~~different time dependent~~across fault flow ~~patterns~~ (Table 2).

Because faults have a smaller offset at their boundaries, and consequently a less distinct damage zone, it was presumed that permeability declines in these areas. This was implemented into the model by using permeability multipliers in the respective elements. The permeability declines linearly towards the ends of the fault, applied to the first and last 15 % of its length. ~~A lateral barrier for groundwater flow due to a low permeable fault core was not considered.~~

3.3 Initial and boundary conditions

In all investigated scenarios, Dirichlet boundary conditions were applied to the Rupelian basal ~~sands~~sand. These were implemented by volume multipliers of 10^{10} at the boundary elements of each layer, so that the aquifer has ~~quasi~~ infinite extension. The boundaries of the Detfurth and the Muschelkalk formations are either open (boundary element volume multiplication by 10^{5}; quasi-infinite) or closed (no boundary element volume multiplication), depending on the

investigated scenario. The higher volume multiplication at the boundary elements of the Tertiary Rupelian basal sand is based on the assumption that a continuous hydraulic connection throughout the formation is more likely in the younger and less consolidated sedimentary deposits than in the more tectonically influenced deeper rocks. For the temperature distribution, a constant geothermal gradient of 30 °C km^{-1} was used, starting from 15 °C at the model top. All simulations were performed at isothermal conditions ~~resulting in a constant initial temperature in time and space. Studies suggest that the salinity in the Rupelian basal sands is between 0.8 % and 3.8 % (Tesch, 1987), and increases with depth until full saturation in the Triassic layers (Hannemann and Schirrmeister, 1998). However, in the present models the transition between freshwater and brine was defined to be abrupt. Here, the Rupelian basal sands contain freshwater (zero salinity), whereas a salinity of 25 % was assigned to all underlying units. These~~. Salinity is assumed to increase with depth either by a gradient of 0.23 g kg^{-1} solution per meter from zero at the base of the Rupelian basal sand up to a maximum of 25 % at a depth of 1070 m (Vattenfall, 2009) or sharply from zero in the Rupelian to 25 % below that aquifer. The last conditions were chosen, as they lead to the maximum possible salinization in the uppermost aquifer, and thus represent the most unfavourable scenario for shallow aquifers under the given assumptions. ~~Furthermore, a sharp salt-freshwater interface serves as a tracer boundary to visualize the distribution of saline water within the shallow aquifer. All simulations were performed at hydrostatic pressure conditions.~~

In the respective industrial project at the Beeskow storage site, it was planned to inject 34 Mt of CO_2 over a time span of 20 years into the Mesozoic formations at the top of an anticline structure (Tillner et al., 2013). In the present study, the equivalent volume of brine was injected into the storage formation instead of CO_2, which enables us to study also the long-term effects of brine displacement more than 1 000 years after the injection stop. Without topographic variations in the reservoir, CO_2 is not immobilized in structural traps (e.g. below an anticline top) and might reach the Fuerstenwalde-Guben fault zone located at a distance of 4 km from the injection well over such a long simulation period, which should not be focus of investigation in the present study. Furthermore, with such a model we keep the findings of injection-related brine displacement transferable to various other types of subsurface storage. All simulations start from hydrostatic pressure conditions. Considering the density of brine, pressure at the top of the Detfurth Formation at 1 425 m depth is approximately 165 bar. At a

reservoir temperature of 58 °C, the resulting CO_2 density is 668.5 kg m^{-3} (Span and Wagner, 1996). Taking into account the salinity of 25 % in the reservoir, brine density is 1 175 kg m^{-3}. Thus, a volume equivalent mass of 59.76 Mt brine was injected into the storage formation, corresponding to a rate of 94.6 kg s^{-1}.

~~At the Beeskow storage site, it was planned to inject 34 Mt of CO_2 over a time span of 20 years into the Mesozoic anticline structure (Tillner et al., 2013). Instead of CO_2, the equivalent volume of brine was injected into the storage formation in the present study, because we assume that there is no substantial impact on resulting brine migration whether CO_2 or water is injected. Furthermore, with such a model we investigate injection related brine displacement, and keep the findings transferable to various other types of subsurface storage. Considering a reservoir pressure of approximately 165 bar at the top of the Detfurth Formation and a temperature of 58 °C, the resulting CO_2 density is 668.5 kg m^{-3} (Span and Wagner, 1996). Brine density sums up to 1 175 kg m^{-3}, taking into account the salinity of 25 %. Thus, a volume equivalent mass of 59.76 Mt brine was injected into the storage formation, corresponding to a rate of 94.6 kg s^{-1}.~~

~~Fluid compressibility is considered in TOUGH2-MP/ECO2N by the use of its density changes, while brine densities are calculated for each element during the simulation.~~Brine densities are calculated in TOUGH2-MP/ECO2N for each element during the simulation and fluid compressibility is then considered by its density changes. Pore compressibility causes a higher storage coefficient in the formations when pressure increases. Since our simulations should show the greatest possible effect on brine displacement, pore compressibility was neglected. ~~Diffusion was also not considered, because it has an irrelevant effect within our model due to the chosen grid discretization and the long timespan it would require to observe substantial effects. If one takes into account a lateral element size of 250 m × 250 m,~~Assuming a fluid diffusion coefficient of 2×10^{-9} m^2 s^{-1} and a sharp freshwater-saltwater interface in the fault, it would take about 1 million years in the present model for the salinity front to propagate into a neighbouring element. We therefore neglected diffusion as well.

4 Set of scenarios

In total, ~~13~~19 scenarios were selected to investigate the conditions for upward brine flow through the faults. ~~Besides~~Different fault lengths~~,~~ and permeabilites, hydrogeological

boundary conditions ~~were varied and~~ and vertical salinity distributions as well as the presence of a ~~potentially overlying~~ secondary reservoir ~~was~~ formation above the target storage horizon were considered. Scenarios are identified by the following abbreviations:

Formatted: English (U.K.)

$$\textit{Scenario} = F_n^{\,l}\, B_{O/C}\, SR_k$$

Where *F* denotes fault with the coefficients *l* indicating the total fault length and *n* the number of active faults. Further, the lateral boundary conditions (*B*) of both reservoirs can be either open (*O*) or closed (*C*). *SR* denotes that an overlying secondary reservoir exists and *k* specifies the permeability of that reservoir. Scenarios in which a salinity gradient was applied are marked with '*'. All simulated scenarios with their varying initial and boundary conditions are summarized in Table 3 and 4.

The base cases consist of two layers, while three different fault lengths were considered. Either all four fault zones with a total length of 193 km were assumed to be permeable, or Fault 1 was defined to be hydraulically conductive with a length of 60 km. In the third case, only a length of 2 kilometres in the central part of Fault 1 was presumed to be open for fluid flow (Fig. 1b). ~~All other parts of~~ Based on the ~~faults were supposed to be impermeable, and therefore consist of inactive elements. These settings represent three different baseline examples, which should distinctly show differences~~effective porosity assumed for ~~a better understanding of~~ all fault zones and the ~~relevant processes, and particularly define~~total fault element volumes, the ~~possible spectrum of brine displacement. Further scenarios considered~~effective damage zone volume for the three different ~~fault lengths described above as well as the Muschelkalk Formation as an overlying secondary reservoir, since multi-barrier systems should preferably be chosen as potential CO_2 injection sites to minimize the risk of leakage.~~cases can be specified with 1.6×10^{10} m^3 (fault length of 193 km), 4.9×10^9 m^3 (fault length of 60 km) and 1.8×10^8 m^3 (fault length of 2 km), respectively. For all these cases, scenarios with both open and closed reservoir boundaries as well as an overlying secondary reservoir were examined to illustrate the entire range of a potential freshwater salinization depending on the given geological constraints.

~~Different fault permeabilities were not considered because previous simulations carried out with closed reservoir boundaries have primarily shown only a temporal effect of fault permeability without any significant change in salinization. The mass of brine displaced into the shallow aquifer was the same in any case irrespective whether the fault permeability was~~

~~higher, equal or lower than the permeability of the secondary reservoir (Fig. 3). A retardation in mass flow into the shallow aquifer by a factor of two was observed only for a fault permeability of 10 mD compared to the base case (700 mD), if all four faults were assumed to be hydraulically conductive. However, one simulation was applied in the present study to investigate the impact of permeability differences between reservoir and faults on upward brine migration taking into account open boundary conditions. In Scenario $F_{1\text{-}4}{}^{193km}B_O\,SR_{2000mD}$, the permeability of the Muschelkalk Formation was increased by one order of magnitude to 2 000 mD, so that in contrast to all other scenarios, the permeability of the secondary reservoir is higher than the fault permeability.~~

5 Results

~~5.1 General outcomes~~

~~Some general outcomes are valid for all simulations. These results are presented first for a better understanding of the system. Figure 4 shows the mass flow in kg s^{-1} as an example for Scenario $F_{1\text{-}4}{}^{193km}B_O$ after 20 years,~~Results of injection induced brine displacement via the faults are analysed at 20 years corresponding to the end of the injection period. At this time, reservoir pressures have reached their maximum, and thus effects on upward brine flow are most noticeable. In Sections 5.2 to 5.5, salinity is assumed to increase sharply from zero in the Rupelian basal sand to 25 % below that aquifer. In Section 5.6, the impact of a salinity gradient on shallower aquifer salinization is presented. Here, salinity in the fault(s) increases from zero at the base of the Rupelian up to a maximum of 25 % at a depth of 1 070 m. Fault permeability is 700 mD in all investigated scenarios, except for the comparison presented in Section 5.4, where duration of mass flow and shallow aquifer salinization are investigated also for lower fault permeabilities of 10 mD and 200 mD. In Section 5.5, it is shown how a secondary reservoir with a permeability higher than that of the faults affects upward brine migration.

5.1 General outcomes~~An~~

In all simulations, an injection-related pattern in pressure distribution and fluid flow can be observed. Figure 3 shows the mass flow of brine as an example for Scenario $F_{1\text{-}4}{}^{193km}B_O$ after 20 years. Starting from the injection location, brine is displaced radially within the reservoir, and hence predominantly into parts of the faults close to the point of injection. ~~Along the~~

~~undulating Fault 3, which is located approximately 30 km away from the injection well, mass flow into parts facing towards the injection can be more than two times higher than into parts of the fault not facing the injection well (Fig. 4). However, the opposite case is noticeable in the shallow aquifer, where flow out of the fault into parts of the aquifer facing away from the injection (lower pressures) is greater than into parts facing it (higher pressures). Hence, a redistribution of fluid flow occurs along the fault. Moreover, an asymmetric flow out of Fault 1 was observed within the Rupelian basal sands. Again, a higher mass flow out of the fault occurs into parts of the aquifer not facing the injection well since brine is displaced away from the point of highest pressurization. Consequently, salinities are higher normal to the fault in areas further away from the injection. This flow behaviour is valid for all scenarios and varies only in its intensity depending on pressure build up and reduction~~However, the course of the four fault zones and the hydraulically conductive fault length impacts fluid flow out of the fault in the shallow aquifer, and thus pressure gradients, so that brine distribution is not symmetric along the faults in the Rupelian basal sand. In case of four open faults, brine that flows out of the faults migrates into the Mittenwalde Block (compartment in the central model domain bounded by the four fault zones; Figure 1) from all four fault zones and towards the open model boundaries. Consequently, pressure gradients are becoming lower in the Mittenwalde Block, so that flow out of all faults towards the lateral boundaries dominates at the final injection stage, since brine is displaced away from the point of highest pressure build-up.

Duration and intensity of fluid flow ~~determines~~determine the spatial distribution of displaced ~~saltwater. Maximum~~ brine. In all scenarios, maximum mass flow ~~was~~is observed along Fault 1 close to the injection point decreasing towards the ~~lateral boundaries of the~~ fault edges. This pattern is reflected in the salinization of the freshwater aquifer, as shown in Figure ~~5a as an example for Scenario $F_{1\text{-}4}^{193km}B_C$.~~4a. A maximum salinity ~~of 23 % is reached within the lower element layer of~~ in the shallow aquifer is reached at the end of the injection period~~, whereas salinity varies only by 5 % to 10 %~~ in the central part of Fault 1, irrespective of whether a sharp salt-/freshwater boundary at the ~~fault edges. Brine migrates upwards through the fault as a result of the injection, and then spreads laterally within the~~ base of the Rupelian ~~basal sands (Fig.~~ (e.g. Scenario $F_{1\text{-}4}^{193km}B_C$) or a salinity gradient (Scenario $F_{1\text{-}4}^{193km}B_C^*$) was applied. Salt concentrations then decrease continuously towards the fault edges by more than 80 %~~,5b).~~ Salinity levels are generally highest within the lower element

Formatted: English (U.S.)

Formatted: Space After: 12 pt

Formatted: Strong, Font color: Black, German (Germany)

layer, indicating that the denser saline water preferably spreads along the base of the aquifer. For the given Scenario $F_{1\text{-}4}^{193km}$ B_C, the saltwater plume width in the Rupelian basal sands reaches a maximum of 2.4 km normal to the central part of Fault 1 and 1.2 km normal to the fault ends (Table 3). For the determination of the lateral distance affected by salinization, only salinities, which exceed 0.05 %, were considered. Due to the reduced (Fig. 4b). Decreasing upward brine displacement after the injection stop, causes a downward flow was observed. The more denseof the denser saline water, which consequently accumulates at the base of the shallow aquifer. Moreover, a slight backflow into the fault occurs due to the increased weight of the water column as a result of the vertical brine displacement. Consequently. Hence, the salinity atin the top element of the faultshallow aquifer slightly decreases by 1.5 % to 23.5 % after a simulated time of 400 a few hundred years (Fig. 5b), and the mass of brine within the fault slightly decreases due to the higher amount of freshwater, what can be observed in the relative mass change within the fault.4b).

Formatted: Font color: Black

5.2 Fault length / effective damage zone volume

The impact of the hydraulic conductive fault length on shallow aquifer salinization is presented in the following. We considered total fault lengths of 2 km, 60 km and 193 km, corresponding to an effective damage zone volume of 1.8×10^8 m^3, 4.9×10^9 m^3 and 1.6×10^{10} m^3, respectively (Table 3).

Figure 5a shows that overpressures in the Detfurth Formation are generally highest assuming laterally closed reservoir boundaries. The pressure development at the base of Fault 1 indicates that pressure increases until the injection stop after 20 years (Fig. 5b).Moreover, the maximum origin depth of the brine displaced into the shallow aquifer was estimated by calculating the fluid flow velocity at the top of the fault. The displaced brine derives from distinctly greater depths close to the injection than at the fault edges (Table 3), e.g. Scenario $F_{1\text{-}4}^{193km}$ B_C shows that close to the injection well, the displaced saline water mainly originates from the upper 30 m of the fault, whereas brine migrates from the upper 3 m at the fault edges only. In all simulations, displaced brine leading to a salinization of the shallow aquifer is displaced only from the upper part of the fault and not originating from the reservoir.

Formatted: Strong, Font color: Black, German (Germany)

5.2 Fault length

5.2.1 Closed reservoir boundaries

Figure 6a shows the distribution of the pressure increase within the upper element layer of the Detfurth Formation for different fault lengths and closed reservoir boundaries. We found the maximum pressure build-up at the injection point to be 89.9 bar for Scenario $F_1^{2km}B_C$, while pressure drops were observed in the surrounding of the faults. As expected, the highest pressure increase within the entire Detfurth Formation was encountered by implementing a hydraulic conductive fault segment with a length of two kilometres only. The pressure increases by 19.4 bar on average until the end of injection period in Scenario $F_1^{2km}B_C$, but only by 4.6 bar when all four faults are open for fluid flow (Table 3). The differences in pressurization of ca. one bar at the base of Fault 1 between scenarios $F_1^{60km}B_C$ and $F_{1-4}^{193km}B_C$ are low compared to the significant differences in total fault length. The pressure development at the base of Fault 1 shows that pressure increases until the injection stops after 20 years (Fig. 6b). In the following, the reduction of pressure is considerably faster, the greater the fault length. If all four faults are open (Scenario $F_{1-4}^{193km}B_C$), fluid flow into the shallow aquifer lasts for about 66 years, and is approximately five times faster than in Scenario $F_1^{2km}B_C$ (Table 3). For result evaluation, only a cumulative mass flow into the Rupelian basal sands above 0.1 kg s^{-1} was taken into account. To retrace and visualize the exchange of fluids between the different units, the relative mass change as a function of time was determined for the different geological units. Figure 7a illustrates that if the reservoir boundaries are closed, the mass of brine displaced into the shallow aquifer corresponds to the overall injected fluid mass. In this case, the open fault length has only a temporal effect on fluid migration.

A higher pressure build-up within the reservoir generally results in higher flow velocities out of the faults. Figure 8 shows the velocity profile through the lower element layer of the Rupelian basal sands. At the end of injection period, flow velocity out of the fault can be up to 29 m yr^{-1} (9.2×10^{-7} m s^{-1}) for a high pressure build-up due to a short fault length of two kilometres ($F_1^{2km}B_C$), while in scenarios $F_1^{60km}B_C$ and $F_{1-4}^{193km}B_C$ flow velocities range between 6.3 m yr^{-1} and 5.8 m yr^{-1} (1.8×10^{-7} m s^{-1}), respectively. Peaks in the velocity profile around the fault refer to the difference in fluid density between the displaced brine and residual freshwater within the aquifer. Maximum flow velocities were observed around

Fault 1, which is located closest to the injection point. Further, velocity increases at the top of all other faults however, not as significantly as observed for Fault 1 (e.g. Fault 3, Fig. 8a). Flow velocities reach a maximum after 20 years. Subsequent to the injection stop, pressure reduction, and lower brine displacement are accompanied by decreasing flow velocities (Fig. 8b).

Freshwater salinization due to displaced brine only occurs locally around the faults. Spatial brine distribution in the Rupelian basal sands reaches a maximum lateral extent of 6.1 km, if a fault of two kilometres length serves as a conductive pathway (Table 3). When Fault 1 is completely open (Scenario $F_1^{60km}B_C$), brine spreads 2.4 km in maximum close to the injection area and only 1.5 km at the fault ends. Differences between the scenarios $F_1^{60km}B_C$ and $F_{1-4}^{193km}B_C$ are low, and mainly expressed by salt concentrations rather than lateral extension. Saline water, which migrates into the Rupelian basal sands, originates only from the fault. The depth of its origin mainly depends on the fault length: in Scenario $F_1^{2km}B_C$ brine is displaced into the shallow aquifer from the upper 298 m of the fault in maximum, while in Scenario $F_{1-4}^{193km}B_C$ saline water rises only 30 m (Table 3).

5.2.2 Open reservoir boundaries

If the reservoir boundaries are open, pressure build up in the Detfurth Formation is considerably lower, while differences corresponding to the fault length still exist. The mean pressure increase within the reservoir is 2.1 bar, if all four faults are open ($F_{1-4}^{193km}B_O$), and hence only half as high as in the scenario with closed reservoir boundaries ($F_{1-4}^{193km}B_C$). In contrary to closed boundary conditions, pressure build up at the model boundary does not occur. A pressure increase of at least one bar was observed in a maximum distance of 58 km ($F_1^{2km}B_O$) and 50 km ($F_{1-4}^{193km}B_O$), respectively, from the injection well. After the stop of injection, the pressure within the reservoir reduces substantially faster than under the assumption of closed reservoir boundaries (Fig. 6b). Hence, the duration of mass flow into the shallow aquifer is shorter for all three scenarios (Fig. 7a). Depending on the open fault length, a significant flow into the shallow aquifer occurs only for 31 years ($F_1^{2km}B_O$ and $F_1^{60km}B_O$) to 42 years ($F_{1-4}^{193km}B_O$). In contrast to closed reservoir boundaries, fluid flow into the Rupelian basal sands is maintained for a longer time period, if all four faults are hydraulically conductive compared to a single fault of only two kilometres length.

~~Due to lower reservoir pressures and the resulting shorter duration of mass flow, the total amount of brine, which is displaced into the shallow aquifer, is reduced in all cases with open reservoir boundaries. As Figure 7b shows, 40 Mt brine reach the Rupelian basal sands when all four faults are open ($F_{1\text{-}4}^{193km}$ B_O), corresponding to 66 % of displaced mass for the same fault length but closed reservoir boundaries ($F_{1\text{-}4}^{193km}$ B_C). The displaced mass of brine is reduced by up to 30 % for a narrow fault of two kilometres length (F_1^{2km} B_O), because a major part of the fluid spreads within the laterally open reservoir (Fig. 7b). After the injection-related upward brine migration stops, a slight backward flow out of the shallow aquifer was additionally observed. Decreasing pressure causes about 3.7 Mt dense fluid to flow out of the Rupelian basal sands back into the fault over a time period of 1 500 years (Scenario F_1^{2km} B_O).~~

In case of a hydraulic conductive fault segment with a length of two kilometres only, brine displacement, and thus pressure dissipation occurs over the smallest area. Consequently, the highest pressure build-up at the injection point (89.9 bar) and the base of Fault 1 (19.0 bar), into which brine is predominantly displaced is observed for Scenario F_1^{2km} B_C (Table 3). A greater effective fault damage zone volume reduces the pressure increase at the base of Fault 1 to 12.1 bar (Scenario F_1^{60km} B_C) and 10.9 bar ($F_{1\text{-}4}^{193km}$ B_C), respectively. Under the assumption of laterally open reservoir boundaries, pressure increase is reduced by a further 23 % in average compared to all three cases with closed boundaries.

Saline water, migrating into the Rupelian basal sand, originates only from the fault(s) and not from greater depth. The higher the vertical pressure gradient, the greater the depth in the fault from which brine is displaced into the shallow aquifer. Hence, in Scenario F_1^{2km} B_C saline water rises into the shallow aquifer from the upper 132 m of the fault, counting from the base of the Rupelian basal sand (Table 3). This maximum displacement depth refers to the central part of Fault 1, where pressure gradients are highest due to the proximity to the injection point. Displacement depths decrease towards the fault edges to partly less than 1 m. The effect of this displacement depth is that the degree in salinization in the Rupelian basal sand becomes locally higher with decreasing effective fault damage zone volume. In Scenario F_1^{2km} B_C, the average salt mass of the area that is affected by a salt concentration exceeding 0.5 g kg^{-1} solution (hereafter referred to as salinization area), which corresponds to the maximum allowable limit prescribed by the German Drinking Water Ordinance (TrinkwV, 2001), is 312 kg m^{-2} after 20 years. In turn, the total salinization area in the Rupelian basal sand is expectably larger the greater the fault length. In Scenario $F_{1\text{-}4}^{193km}$ B_C, this area is more

than seven times as large as in Scenario F_1^{2km} B_C (Table 3). However, the salt mass per unit area is considerably lower, since pressure dissipation occurs over a greater hydraulic conductive fault length, which reduces pressure gradients and brine displacement depths in the faults (30 m in Scenario F_1^{60km} B_C and 29 m in Scenario $F_{1\text{-}4}^{193km}$ B_C). Thus, the average salt mass of the salinization area in the Rupelian basal sand is 141 kg m^{-2} in Scenario F_1^{60km} B_C and 84 kg m^{-2} in Scenario $F_{1\text{-}4}^{193km}$ B_C. Lower vertical pressure gradients in the fault in case of laterally open reservoir boundaries reduce brine displacement depths and flow velocities out of the faults, respectively, and consequently the size of the salinization areas and average displaced salt masses in the Rupelian basal sand compared to the scenarios with closed reservoir boundaries (Fig. 6).

After the injection stop, fluid flow persists until the overpressure in the storage formation is completely reduced. Duration of fluid flow and pressure reduction thereby depend on the lateral boundary conditions and the hydraulically conductive fault length. Pressure reduces substantially faster with increasing fault length and under the assumption of laterally open fluid flow boundaries that allow for horizontal brine displacement across the model boundaries (Fig. 5b). Hence, the duration of brine displacement into the shallow aquifer is shorter for all three scenarios. After 31 years (Scenario F_1^{2km} B_O) to 42 years (Scenario $F_{1\text{-}4}^{193km}$ B_O), pressure conditions prior to injection are re-established (Fig. 7a). In case of closed reservoir boundaries, pressure reduction in the incompressible domain solely comes from vertical brine displacement via the fault(s) towards the laterally infinite shallow aquifer. Thus, under the assumption of a sharp salt-freshwater boundary, the mass of salt displaced into the shallow aquifer corresponds to the overall injected salt mass (Fig. 7b). In this case, the open fault length affects only the duration of fluid migration, which can be between 66 years (Scenario $F_{1\text{-}4}^{193km}$ B_C) and 330 years (Scenario F_1^{2km} B_C); (Fig. 7a). Decreasing vertical pressures after upward brine migration stops at the end of injection, cause a slight backward flow of brine out of the shallow aquifer and back into the fault in case of a small effective fault damage zone volume and laterally open reservoir boundaries. Over a period of 300 years, the average salt mass in the Rupelian decreases by about 7.5 x 10^8 kg salt (Scenario F_1^{2km} B_O).

5.3 Overlying secondary reservoir

~~5.3.1 Closed reservoir boundaries~~

~~An overlying~~A secondary reservoir above the storage formation also hydraulically connected to the fault zones has a strong impact on pressure build-up within the injection horizon~~.~~, and hence vertical pressure gradients in the fault(s). If ~~all~~ reservoir boundaries are closed for fluid flow, the ~~mean~~ pressure increase ~~within~~at the ~~Detfurth Formation~~base of Fault 1 ranges from ~~15.~~9.0 bar (F_1^{2km} B_C SR_{200mD}) to ~~2.9~~6.4 bar ($F_{1\text{-}4}^{193km}$ B_C SR_{200mD}~~) in correspondence~~), which corresponds to ~~80~~48 % and ~~63~~59 % of the pressure increase, respectively, without considering the overlying secondary reservoir. Under the assumption of laterally open reservoir boundaries, pressure increase is again reduced by further 24 % in average, compared to all three cases with secondary reservoir and closed boundaries. This results in the lowest vertical pressure gradients in the fault(s) observed in the present scenario analysis. Lower reservoir pressures due to an overlying secondary reservoir induce lower flow velocities out of the fault as well as shown in Figure 8. Moreover, brine displaced into the Rupelian basal sand originates from considerably shallower depths in the fault. Here, brine is displaced into the Rupelian basal sand from the upper 70 m of Fault 1 in Scenario F_1^{2km} B_C SR_{200mD} and 17 m in Scenario $F_{1\text{-}4}^{193km}$ B_C SR_{200mD} considering laterally closed reservoir boundaries. Under the assumption of open flow boundaries, brine mainly originates from the upper 56 m (Scenario F_1^{2km} B_O SR_{200mD}) and 16 m (Scenario $F_{1\text{-}4}^{193km}$ B_O SR_{200mD}) of the faults only. Consequently, the area affected by a salt concentration exceeding 0.5 g kg^{-1} solution in the Rupelian basal sand as well as the average salt mass in the salinization area are reduced by about one third compared to the respective scenario without considering a secondary reservoir (Table 3). ~~After the injection period,~~Again, pressure conditions prior to injection re-establish fast after the injection stop and under the assumption of laterally open reservoir boundaries (e.g., 40 years for Scenario F_1^{60km} B_O SR_{200mD}); (Fig. 9). In turn, the reduction of the comparatively lower overpressures takes significantly ~~longer~~more time in case of laterally closed reservoir boundaries, e.g.~~.~~., the mass flow into the Rupelian basal ~~sands takes place~~sand continuous for about ~~1 050 years (F_1^{2km} B_C SR_{200mD}) and~~ 225 years ($F_{1\text{-}4}^{193km}$ B_C SR_{200mD}) and 1 050 years (F_1^{2km} B_C SR_{200mD}), which is more than three times longer compared to the models without a secondary reservoir~~. Figure 9 illustrates the explanation for this flow retardation: During the injection, fluid is displaced within the Detfurth Formation, and further through the faults into the Muschelkalk Formation (Fig. 9a). Due to the successive pressure reduction~~ (Fig. 10). This

Formatted: Space Before: 0 pt

retardation in fluid flow is attributable to the fact that the overpressure in both ~~reservoirs, brine is transported out of the respective reservoir afterwards (Fig. 9b). This retardation can be clearly observed in~~, injection horizon and secondary reservoir is successively reduced after the injection stop. According to the ~~mass balances, comparing the displaced brine mass into the~~ pressure gradient towards the Rupelian basal ~~sands for the scenarios~~sand with ~~and without an overlying~~ laterally infinite extension, brine is displaced out of the secondary reservoir again after the injection stop and into the shallow aquifer (Fig. 11). ~~9c). However~~Thus, the overall displaced ~~brine~~salt mass ~~into~~in the shallow aquifer is almost identical compared to the corresponding scenarios without secondary reservoir, when pressure comes to an equilibrium (Fig. 10). ~~Nevertheless,~~

5.4 Fault permeability

To evaluate the impact of fault permeability on upward brine displacement via the existing faults, a comparison was made between six scenarios that consider an effective damage zone volume of 1.6 x 10^{10} m^3 (total fault length of 193 km) and a fault permeability of 10 mD, 200 mD and 700 mD for ~~a short~~laterally open ~~fault of two kilometres (F_1^{2km} B_C SR_{200mD}) it takes a long~~and closed reservoir boundaries, respectively. Figure 12 and Table 4 show that the relative salt mass change in the Rupelian basal sand at the injection stop is almost identical for a fault permeability of 700 mD and 200 mD. Thereby, laterally open model boundaries reduce the average salt mass of the salinization areas in the Rupelian basal sand by about 12 % compared with the models using laterally closed boundaries. A less permeable fault with a permeability of 10 mD has a more significant impact on the degree of upper aquifer salinization. The relative salt mass change in the Rupelian basal sand after 20 years is 17 % lower in average compared with a fault permeability of 200 mD or 700 mD. However, in a laterally closed and incompressible domain all the pressure relief comes from upward brine migration. Consequently, all the injected brine volume reaches the shallow aquifer after a certain time since flow persists until the ~~pressure conditions prior to injection are re-established, although pressure differences are already low.~~ overpressure in the storage formation is completely reduced. In this case, a low-permeable fault only extends the duration of mass flow into the shallow aquifer, which can persist up to 310 years (Fig. 12; Table 4). At that time, the total salt mass displaced into the Rupelian basal sand is the same as for the scenarios with a fault permeability of 200 mD or 700 mD.

Formatted: Space After: 12 pt, Tab stops: Not at 7 cm

Formatted: Font color: Black

Due to lower reservoir pressures, flow velocities are lower as well. This is particularly obvious for Scenario F_1^{2km} B_C SR_{200mD}, where flow velocity out of Fault 1 is halved at the end of the injection period compared to the scenario without the overlying secondary reservoir (Fig. 11). However, because the displaced brine mass becomes equal in both scenarios after a certain period of time, the area affected by salinity increase in the Rupelian basal sands is comparable to that observed in the simulations considering only two model layers (Table 3). Because of the delay in mass flow due to the existence of an overlying reservoir, the injection related pattern occurs damped, and a more even distribution of saltwater in the shallow aquifer was observed. This is especially the case for the scenarios with greater fault length (F_1^{60km} B_C SR_{200mD} and $F_{1\text{-}4}^{193km}$ B_C SR_{200mD}): Salinity and width of the displaced brine normal to the fault are slightly reduced closer to the injection well, while comparatively higher values can be observed at a greater distance to the point of injection.

5.3.2 Open reservoir boundaries

Open reservoir boundaries and an overlying secondary reservoir result in the lowest pressure build up within the Detfurth Formation. The mean pressure increase in the reservoir ranges from 3.2 bar (F_1^{2km} B_O SR_{200mD}) to 1.3 bar ($F_{1\text{-}4}^{193km}$ B_O SR_{200mD}), corresponding to 16 % and 28 % of the pressure increase, respectively, without taking into account the overlying secondary reservoir (Table 3). A pressure increase of at least one bar was observed at a maximum distance of 55 km (F_1^{2km} B_O SR_{200mD}) and 40 km ($F_{1\text{-}4}^{193km}$ B_O SR_{200mD}) from the injection well, depending on the open fault length. After the injection stop, pressure decreases much faster than in all other scenarios. The overlying secondary reservoir leads to a smaller retardation in fluid flow only, which is not comparable to the observed delay if reservoir boundaries are closed. Duration of mass flow into the shallow aquifer ranges between 31 years (F_1^{2km} B_O SR_{200mD}) and 45 years ($F_{1\text{-}4}^{193km}$ B_O SR_{200mD}). A backflow out of the shallow aquifer was observed as well (Fig. 12).

The flow velocity out of the two kilometres long fault shows its maximum of 10 m yr^{-1} at the end of the injection period. For the scenarios F_1^{60km} B_O SR_{200mD} and $F_{1\text{-}4}^{193km}$ B_O SR_{200mD}, flow velocities are only slightly lower, and decrease marginally faster than in the simulations with closed boundaries (Fig. 11). The mass of brine displaced upward into the shallow aquifer is further reduced. Taking into account the backflow after 1 000 years, only 7.2 Mt of brine are transported into the Rupelian basal sands for a fault length of two kilometres

~~(F_1^{2km} B_O SR_{200mD}). This corresponds to 12 % of the mass which reaches the shallow aquifer when reservoir boundaries are closed and no secondary reservoir exists (F_1^{2km} B_C). The major part of the displaced fluid spreads within the laterally open Detfurth Formation. For greater fault lengths, also the mass brine migrating into the Rupelian basal sands is lower: here, only 27 % (F_1^{60km} B_O SR_{200mD}) and 33 % ($F_{1\text{-}4}^{193km}$ B_O SR_{200mD}) of the injected mass is displaced into the freshwater aquifer, respectively (Fig. 12). For these scenarios, a higher amount of brine spreads within the Muschelkalk Formation.~~

~~Hence, due to the significantly lower brine displacement into the shallow aquifer, also the lateral brine extension is minor. In the Rupelian basal sands, the salinity increases up to a distance of 2.8 km around the fault with a length of two kilometres (F_1^{2km} B_O SR_{200mD}). This is less than half the extension compared to the scenario with closed reservoir boundaries and considering only two model layers (F_1^{2km} B_C). Moreover, the brine, which is displaced into the freshwater aquifer, originates from considerably shallower depths: for a fault length of two kilometres (F_1^{2km} B_O SR_{200mD}) the brine rises in the extreme from the upper 59 m of the fault. In the case with four open faults, ($F_{1\text{-}4}^{193km}$ B_O SR_{200mD}) brine mainly originates from the upper 17 m of the faults.~~

~~5.4~~5.5 Permeability ~~differences~~difference between ~~the~~ fault and secondary reservoir

Our ~~previous~~ simulations demonstrate that if reservoir boundaries are closed, the permeability of the fault ~~only has a temporal impact on~~primarily influences the duration of fluid flow ~~only, and~~. After a certain period, the overall displaced ~~brine~~salt mass into the freshwater aquifer becomes equal ~~after a certain period~~, if fault zones are sufficiently permeable. For this case, it is irrelevant if fault permeability is higher, equal or lower compared to the reservoir or aquifer. This is not ~~the case if the~~ true for open reservoir flow boundaries ~~are open~~ (infinite aquifer).

In Scenario $F_{1\text{-}4}^{193km}$ B_O SR_{2000mD}, the permeability of the Muschelkalk Formation is distinctly higher than that of the fault. The ~~mean reservoir~~ pressure ~~increases by less than half (0.6~~ increase at the base of Fault 1 is only 1.2 bar~~) compared~~, which corresponds to 23 % of the ~~scenario with~~total pressure increase, considering a Muschelkalk Formation permeability of ~~only~~ 200 mD ($F_{1\text{-}4}^{193km}$ B_O SR_{200mD}). ~~In addition, the total duration of mass flow into the Rupelian basal sands is lowest with only 23 years compared to all other scenarios. However,~~

Formatted: Space Before: 0 pt

Formatted: Space After: 6 pt

~~in this scenario brine preferentially migrates into the permeable Muschelkalk Formation and not into the shallower aquifer. As illustrated in Figure 13, most of the injected brine is displaced into the overlying secondary reservoir, and only 3.5 Mt remain in the Detfurth Formation. The mass of saline water transported into the Rupelian basal sands is only 5.5 Mt, corresponding to 9 % of the total injected mass.~~ In consequence, ~~salinization of the Rupelian basal sands is lowest, and the extent of the displaced brine smallest in this scenario compared to all others (Table 3). Moreover, the fluid~~brine that is displaced into the shallow aquifer originates solely from the upper 4 m of the faults. This results in the smallest salinization area and the lowest degree in salinization in the Rupelian basal sand compared to all other scenarios with a sharp salt-/freshwater boundary (Fig. 13; Table 3). In addition, the shortest duration of mass flow into the Rupelian basal sand with only 23 years is observed for Scenario $F_{1\text{-}4}^{193km}\ B_O\ SR_{2000mD}$.

5.6 Salinity gradient

Two further scenarios, considering a total fault length of 2 km (Scenario $F_1^{2km}\ B_C^*$) and 193 km (Scenario $F_{1\text{-}4}^{193km}\ B_C^*$), without an overlying secondary reservoir and laterally closed reservoir boundaries were employed to investigate the impact of a salinity gradient on the degree of shallow aquifer salinization. The pressure increase at the base of Fault 1 is almost identical comparing both scenarios with the corresponding scenario exhibiting a sharp salt-/freshwater boundary below the Rupelian. Thus, a significant difference in the brine displacement depth in the faults cannot be observed after 20 years (Table 3). The displacement depth in the fault(s) is 132 m for Scenario $F_1^{2km}\ B_C^*$ and 29 m for Scenario $F_{1\text{-}4}^{193km}\ B_C^*$, respectively. Consequently, the mass of brine displaced into the shallow aquifer after 20 years is very similar with 2.2 x 10^{10} kg (Scenario $F_1^{2km}\ B_C^*$) and 2.5 x 10^{10} kg (Scenario $F_1^{2km}\ B_C$), as well as 4.1 x 10^{10} kg (Scenario $F_{1\text{-}4}^{193km}\ B_C^*$) and 4.9 x 10^{10} kg (Scenario $F_{1\text{-}4}^{193km}\ B_C$). However, salt concentrations of brine that is displaced out of the fault(s) and into the shallow aquifer are significantly lower when taking into account a salinity gradient instead of a sharp salt-/freshwater interface. Hence, the average salt mass of the salinization area in the Rupelian basal sand is only 9 % (Scenario $F_1^{2km}\ B_C^*$) and 12 % (Scenario $F_{1\text{-}4}^{193km}\ B_C^*$) of that in the respective scenarios with the sharp salt-/freshwater boundary (Fig. 14; Table 3).

6 Discussion

The analysis of all scenarios provides both, general outcomes for a better understanding of the relevant processes and the impact of all investigated parameters as well as site-specific findings. In a previous study, Tillner et al. (2013) demonstrated that pressure build up in the reservoir is the driving factor in upwards brine migration: Larger pressure build up leads to stronger brine displacement, and consequently higher salinities in shallow aquifers. Our simulations confirm these observations. Moreover, we have shown that the magnitude of pressure build up induced by fluid injection and its release strongly depends on the choice of lateral boundary conditions, the effective damage zone volume of faults and the presence of secondary reservoirs. The maximum pressure increase of 19.4 bar in average within the reservoir occurs if the reservoir boundaries are closed, no overlying secondary reservoir exists, and the hydraulically conductive fault segment is short (F_1^{2km} B_C). This results in the highest observed flow velocities of 29 m yr^{-1} for Fault 1. Consequently, the displaced brine spreads 6.1 km laterally around the fault within the shallow aquifer in the extreme. Moreover, the spatial distribution of pressure build up leads to an injection related pattern in fluid flow, resulting in higher salinities within the Rupelian basal sands above fault intervals, which are located closer to the injection well. However, we neglected pore compressibility in our models to maximize pressurization and subsequent brine displacement. Considering pore compressibility, would lead to a slight reduction in injection related pressure build up due to higher storage coefficients in the formations, and consequently to less intense brine displacement during the injection period.

All simulations with closed reservoir boundaries that correspond to a spatially restricted reservoir further show that the mass of brine displaced into the shallow aquifer corresponds to the overall injected mass. For that reason, fluid flow persists until the injection related overpressure within the reservoirs is completely vanished. Hence, only a temporal effect on upward brine migration depending on fault length and the presence of an overlying reservoir was observed in this case. For a fault segment of two kilometres length (F_1^{2km} B_C) the flow into the shallow aquifer can last up to five times longer than for the scenario with four open faults (F_{1-4}^{193km} B_C). Thereby, the presence of an overlying secondary reservoir results in fluid flow retardation by factor 3.1 to 3.4 in the scenarios F_1^{2km} B_C SR_{200mD} and F_{1-4}^{193km} B_C SR_{200mD}, respectively. Open reservoir boundaries represent an aquifer with a quasi infinite extension and allow lateral pressure dissipation. As a result, substantially lower pressures within the

Detfurth Formation and a reduction of shallow aquifer salinization can be observed. Consequently, only 66 % of the brine mass is displaced into the shallow aquifer assuming four open faults ($F_{1\text{-}4}^{193km}$ B_O) and about 30 % in the two kilometres single fault case (F_1^{2km} B_O) in comparison to the corresponding scenarios with closed faults. The presence of an overlying secondary reservoir leads to an additional decrease in salinity: 33 % and 12 % of equivalent brine mass migrates into the shallow aquifer in the scenarios $F_{1\text{-}4}^{193km}$ B_O SR_{200mD} and F_1^{2km} B_O SR_{200mD}, respectively. These results illustrate the relevance of representing the site specific geological conditions as close as possible, as previously proposed by e.g. Cavanagh and Wildgust (2011).

As mentioned above, the results of the investigated scenarios emphasize that also the effective volume of the hydraulically conductive length of the fault zones has an important influence on pressure build up and release in geological underground utilization. Depending on the fault length, also the duration and intensity of the mass flow varies, in turn determining the overall salinization of a shallow aquifer. A short hydraulically conductive fault segment leads to higher reservoir pressures and a wider salinization locally around the fault (F_1^{2km}) than a fault that is open over its entire length ($F_{1\text{-}4}^{193km}$), because pressure dissipation occurs across a smaller area. Based on our definition, that the fault is either permeable (open) or impermeable (closed) for fluid flow, the location of potential salinization is pre determined. Hence, the open fault length affects both, the location and degree of the occurring salinization. Moreover, these influences correspond not only to fault length, but also to fault width, since porosity was maintained constant during all our simulations. Thus, the effective damage zone volume of hydraulically conductive faults is relevant for the simulation outcome.

Tillner et al. (2013) showed that the permeability of fault zones only has a minor impact and does not influence salinization of shallower aquifers significantly. The authors considered mainly fault permeabilities higher than that of the reservoirs. Our previous simulations have also primarily shown a temporal effect of fault permeability without any significant change in salinization assuming closed reservoir boundaries. Furthermore, our results demonstrate that the relation between fault and reservoir permeability has a crucial impact on salinization of upper aquifers assuming a laterally infinite reservoir extension. In Scenario $F_{1\text{-}4}^{193km}$ B_O SR_{2000mD}, it is shown that fault permeability lower compared to that of the secondary reservoir, determines the preferential brine flow direction. If permeability of the secondary reservoir exceeds that of the fault, the mass of brine migrating into the Rupelian

~~basal sands is only around a quarter of that observed in the opposite case ($F_{1\text{-}4}^{193km}$ B_O SR_{200mD}).~~

~~Simulations taking into account an overlying secondary reservoir result in considerably lower pressures in the storage reservoir. Moreover, a dampening effect on salinization of the shallow aquifer occurs, because fluid is partially displaced into this layer, and thus further brine displacement upward the fault is reduced. Hence, it can be assumed, that the potential salinization of a shallow aquifer is lowered with each aquifer lying in between the reservoir and the shallow aquifer. Similar results were achieved by an analytical approach of Nordbotten et al. (2004), investigating fluid leakage through wells in a multi-barrier system with up to 12 aquifers. The authors observed a successive decrease in intensity of fluid upward displacement, caused by loss of fluid into the intermediate aquifer layers, what consequently highly reduces leakage in the shallowest aquifer.~~ The present study demonstrates how the presence of regional faults can affect upward brine displacement and the degree of shallow aquifer salinization in geological underground utilization. Different fault permeabilites, effective damage zone volumes, hydrogeological boundary conditions and vertical salinity distributions as well as the presence of a secondary reservoir formation above the target storage horizon are considered in a comprehensive large-scale scenario analysis. A 3D geological model of a potential onshore storage site in the Northeast German Basin serves as the basis for this research. The results emphasize that maximum vertical pressure gradients in faults are observed for closed reservoir boundaries, if no overlying secondary reservoir exists and the effective fault damage zone volume is relatively small. The higher the vertical pressure gradient, the greater the depth in the faults from which brine is displaced into the shallow aquifer. A large effective fault damage zone volume, open reservoir boundaries and a secondary reservoir above the storage formation, also hydraulically connected to the fault zones, significantly reduce pressure gradients, and thus displacement depths in the fault. These range between 132 m (Scenario $F_1^{2km}{}_{BC}$) and 4 m ($F_{1\text{-}4}^{193km}$ B_O SR_{2000mD}) after 20 years of fluid injection, respectively. Consequently, salt concentrations in the shallow aquifer are higher in the fault vicinity, the smaller the effective fault damage zone volume. The degree in salinization thereby strongly depends on the initial salinity distribution in the fault. If salinity increases sharply from, e.g., zero in the shallow aquifer to 25 % below its base, the average salt mass of the area affected by salinization amounts to 312 kg m^{-2} after 20 years of injection (Scenario $F_1^{2km}{}_{BC}$). A salinity gradient of 0.23 g kg^{-1} solution per meter reduces the average

salt masses of the salinization area in the shallow aquifer by more than 90 % to 28 kg m^{-2} (Scenario $F_1^{2km}{}_{BC}^{*}$). On the contrary, the salinization area in the shallow aquifer, assuming a total hydraulically conductive fault length of 193 km is seven times larger than for a fault length of 2 km. However, lower pressure gradients and brine displacement depths in the fault decrease the degree in salinization in the shallow aquifer, since pressure dissipation occurs over a larger area.

In all scenarios, salinization in the shallow aquifer was observed only along and in close proximity to the open fault zones up to a lateral extent of 2 km (Scenario $F_1^{2km}{}_{BC}$; small effective fault damage zone volume) to a few hundred meters ($F_{1\text{-}4}^{193km}\ B_O\ SR_{200mD}$; large effective fault damage zone volume and secondary reservoir) from the fault. Brine that reaches the shallow groundwater system ~~Birkholzer et al. (2009) also showed, however, without considering a vertical conduit that the amount of fluid displaced into formations above the reservoir, decreases upwards due to the attenuation capacity of the overlying rocks.~~

~~For the given geological conditions and the assumed injection rate, the fluid displaced into the shallow aquifer originates solely from the upper part of the fault. Depending on the scenario, brine displaced into the shallow aquifer originates from the upper 4 m ($F_{1\text{-}4}^{193km}\ B_O\ SR_{2000mD}$) to 298 m ($F_1^{2km}\ B_C$) of the part of Fault 1 lying close to the injection, while the depth of brine origin is substantially reduced up to less than 1 m at fault edges. Consequently, the initial distribution of salinity within the fault is crucial for the assessment of shallow aquifer salinization. Our simulations with a fault fully saturated with brine correspond to an end member resulting in a maximum freshwater salinization. In this case, a small conductive fault segment would lead to higher salinities and a greater lateral propagation of the saltwater, while faults with a great effective damage zone volume lead to a more distributed salinization but lower spatial widths of the saltwater distribution. If, however, a gradient in salinity exists or the salt-freshwater interface lies below the depth, from which brine is displaced into the shallow aquifer, freshwater salinization is considerably reduced or might not occur. Nevertheless, if the displaced brine reaches the shallow groundwater system it~~ spreads preferentially at the aquifer base, as indicated by considerably higher salinities at the lower element layer in ~~the Rupelian basal sands. These results are in~~our simulations, which is in good agreement with the findings of Oldenburg and Rinaldi (2011).

~~Our simulation results also show that~~ Oldenburg and Rinaldi (2011) further show that upward flux into the bottom-most part of the shallow aquifer is sustained until a new hydrostatic equilibrium is reached, if the pressure elevation is high enough and the dense brine can spread unhindered in the upper aquifer. Our simulation results based on closed reservoir boundaries confirm these results. The mass of brine displaced into the shallow aquifer corresponds to the overall injected mass after several tens to hundreds years, since the duration of brine displacement into the shallow aquifer is not limited to the injection period~~. Even in the scenario assuming~~ only. Laterally open reservoir boundaries and ~~four hydraulically conductive faults ($F_{1\text{-}4}^{193km}$ B_O), both supporting~~a large effective fault damage zone volume support a fast pressure reduction, however brine displacement into the shallow aquifer persists for more than twice the injection period. ~~This illustrates~~Under the assumption of closed reservoir boundaries, all pressure relief results from upward brine migration via the faults. In this case, a small effective fault damage zone volume or a low permeable fault only extend the duration of brine flow into shallower units, so that fluid flow can persist for more than 1 000 years until the overpressure in the storage formation is completely reduced, resulting in an ongoing salinization far beyond the time of the injection stop. This demonstrates the relevance of considering also the post-injection phase in salinization assessments, since neglecting the ongoing fluid flow processes could lead to an underestimation of the potential freshwater salinization. ~~Moreover, it is important to recognize further post injection processes, as the observed density-driven flow out of the shallow aquifer back into the faults occurring due to the increased weight of the water column~~Nevertheless, it should be noted that regional groundwater flow and mixing with local recharge would probably have a strong effect on the reduction of salt concentrations in the shallow aquifer over a period of several hundred years. As demonstrated by the results, it is crucial to represent the site-specific geological conditions as close as possible. Cavanagh and Wildgust (2011) point out that storage formations are unlikely to have zero-flow boundaries and are rather open with respect to single-phase flow and pressure dissipation via brine displacement at regional scale~~.~~.

In a previous study focussing on the same storage site, Tillner et al. (2013) demonstrated that increasing fault permeability from 100 mD to 10 000 mD does not significantly affect the degree in shallow aquifer salinization. Our simulations further show that only low fault permeability has a significant impact on upward brine migration. Depending on the lateral reservoir boundaries, the relative salt mass change in the shallow aquifer after 20 years is 13-

Formatted: English (U.S.)

22 % lower for a fault permeability of 10 mD compared with a fault permeability of 700 mD. Tillner et al. (2013) mainly considered fault permeabilities higher than that of the reservoir and overlying permeable formations. Our simulations demonstrate that the preferential brine flow direction, and thus salinization of upper aquifers is determined by the permeability contrast between fault and reservoir and/or overlying secondary reservoirs. If permeability of an overlying secondary reservoir exceeds that of the fault ($F_{1\text{-}4}^{193km}\ B_O\ SR_{2000mD}$), the mass of brine migrating into the shallow aquifer is only around a quarter of that observed in the opposite case ($F_{1\text{-}4}^{193km}\ B_O\ SR_{200mD}$). Thus, it can be concluded that in multi-barrier systems the potential salinization of a shallow aquifer is lowered with each intermediate aquifer, if a hydraulic connection exists between the fault or leakage pathway and that aquifer. Similar results were achieved by an analytical approach of Nordbotten et al. (2004), investigating fluid leakage through wells in a multi-barrier system with up to twelve aquifers. The authors observed a successive decrease in the intensity of upward fluid displacement, caused by the migration of fluid into the intermediate aquifer layers, consequently reducing fluid migration in the shallowest aquifer. Birkholzer et al. (2009) also showed that the amount of fluid displaced into formations above the reservoir decreases in upward direction due to the attenuation capacity of the overlying rocks; however, without considering a vertical conduit. Further, Walter et al. (2012) concluded that saltwater intrusion into potable groundwater resulting from geological CO_2 storage in a saline aquifer occurs most likely in the vicinity of vertical fluid conduits and not over large areas, if sites with multi barrier systems and intermediate aquifers are selected. Zeidouni (2012) evaluated vertical communication between aquifers through a leaky fault by an analytical approach and showed that the attenuation capacity of a single, thick overlying aquifer is distinctly smaller than that of a multi-layered system.

In the present study, a conservative modelling approach in the assessment of potential upper aquifer salinization by upward brine migration from saline formations was chosen. We injected brine instead of CO_2 and neglected pore compressibility in our models to maximize pressurization and related brine displacement. Considering the effects of CO_2 and/or pore compressibility, would induce a lower injection-related pressure-build up due to higher storage coefficients, and consequently to less intense brine displacement in the injection period. Furthermore, our simulations with a fault fully saturated with brine correspond to an end member resulting in maximum freshwater salinization. Brine migration across the faults

is possible, since no impermeable fault core was considered; however, brine migration occurs almost solely upward into the overlying formations and is negligible in horizontal direction across the faults, when applying a higher fault than reservoir permeability. Hence, the presented modelling results are valid for one specific fault architecture promoting vertical fluid flow, as a least favourable case with respect to shallow aquifer salinization. In multi-layer systems with alternating layers of reservoirs and caprocks, as that considered in the present study, fault permeability within the caprock layers is usually lower than that of the fault host rocks resulting from the clay smearing effect (e.g. Crawford et al., 2008; Egholm et al., 2008). Fault permeability varies not only with mineralization along the fault plane, but also with e.g., depth, fault throw and orientation, inducing highly heterogeneous horizontal and vertical permeability patterns (e.g., Vilarrasa and Carrera, 2015; Bense and Person, 2006; Odling et al., 2004; Shipton et al., 2003; Fisher and Knipe, 2001). Heterogeneity in fault permeability can prevent brine from migrating in upward direction and result in much lower salt concentrations or a differently distributed salinization pattern in the shallow aquifer as presented here. However, hydraulic properties and the spatial extent of fault damage zones are difficult to detect and therefore exhibit a high uncertainty in predicting fault fluid flow and potentially resulting shallow freshwater salinization (Odling et al., 2004; Harris et al., 2003). Further, geomechanical effects are relevant in the assessment of fault fluid flow and several authors have explored the impact of injection-induced pressure build-up on fault zones stability (e.g., Kempka et al., 2015; Rinaldi et al., 2015; Tillner et al., 2014; Magri et al., 2013; Röhmann et al., 2013; Cappa and Rutqvist, 2011~~Finally, we can complement our general findings with site-specific insights: For the study area, the presence of overlying reservoirs, represented by the Hardegsen, Muschelkalk and Stuttgart formations, as well as the initial gradient in salinity are known. This gradient reduces the potential salinization, because the fluids displaced into the Rupelian basal sands would be of essentially lower salinity than assumed in our simulations. Based on these results, it can be concluded that for a large effective damage zone volume (as in Scenario $F_{1\_4}^{193km}$), shallow aquifer salinization is estimated as low, even if fluid is displaced over extensive areas into the Rupelian basal sands, because the origin depth of these fluids lies in maximum only a few decametres below the shallow aquifer. At the same time, local and very permeable segments of the fault (as in Scenario F_1^{2km}) affect a higher vertical distance by upward brine migration, resulting in a higher potential for possible freshwater salinization. Furthermore, according to the present~~

~~study, we are convinced that the three interlayered reservoirs would dampen brine displacement into the shallow aquifers, because fluids would be partly displaced into these layers instead of further migrating upwards.~~

). For this purpose, coupled hydro-mechanical simulations are applied to account for the interaction between hydraulic and mechanical processes, potentially triggering fault slip and dilation resulting in, e.g., new or enhanced leakage pathways for formation fluids. To minimize pressure perturbation due to fluid injection, and thus fault fluid flow, simultaneous fluid injection and production from storage reservoirs is discussed as one efficient mitigation measure to be applied in geological underground utilization (Kempka et al., 2014; Tillner et al., 2013; Court et al., 2012; Bergmo et al., 2011; Buscheck et al., 2011).

For future investigations, we extend the assumptions made in the present study by the implementation of heterogeneous fault zones with spatial variations in porosity and permeability as well as related non-uniform architecture and fault inclination. Furthermore, research is underway to implement the 3D model presented here in coupled hydro-mechanical simulations to account for potential fault shear failure and permeability changes that may alter fault fluid flow.

7 Summary and Conclusions

~~In the present study, a~~A regional scale 3D model ~~(100 km × 100 km × 1.34 km)~~ of the prospective storage site Beeskow in the Northeast German Basin was implemented to investigate ~~a~~the potential salinization of potable groundwater resources ~~due to~~, resulting from upward brine migration through hydraulically conductive fault zones. For that purpose, ~~13~~19 scenarios were examined to assess the impact of fault lengths between 2 km and 193 km in the vicinity and around the injection ~~site~~location. Further, the effects of an overlying secondary reservoir ~~as well as the geological~~, hydrogeological boundary conditions ~~on~~and the initial salinity distribution on freshwater salinization ~~of a shallow aquifer~~ were evaluated.

We ~~have shown~~demonstrate that pressure build-up and ~~its~~ development ~~over time~~ within the reservoir determine the intensity and duration of fluid flow through the faults~~,~~ and ~~thereby the~~shallow aquifer salinization ~~of shallower aquifers. Thereby, the total mass of brine displaced into the uppermost aquifer essentially depends on the chosen geological boundary conditions: if reservoir boundaries are closed, representing a spatially restricted reservoir, the fluids migrating into the shallow aquifer correspond to the overall injected fluid mass~~

~~(assuming zero pore compressibility). Only a temporal effect was observed on the retardation of fluid flow for shorter open fault lengths and the presence of an overlying secondary reservoir. If reservoir boundaries are open, corresponding to an aquifer with quasi infinite extension, freshwater salinization is considerably reduced. With a secondary reservoir, only 12 % of equivalent brine mass migrates into the shallow aquifer for a hydraulically open fault segment of two kilometres.~~

~~The initial salinity distribution~~ , mainly controlled by the lateral model boundary settings and ~~location of the fresh saltwater interface within the upper part of the fault is of high relevance for risk assessment related to salinization in shallow aquifers. For the considered geological conditions, the fluid displaced into the uppermost aquifer originates in maximum from the upper 4 m to 298 m of the investigated faults. Hence, if the salt-freshwater interface lies below this depth, no salinization is likely to occur, since only freshwater would be displaced into the shallow aquifer.~~the effective fault damage zone volume. In general, the potential of freshwater salinization is ~~small~~low for greater effective fault damage zone volumes or fault lengths, because the origin depth of the fluids displaced into the shallow aquifer ~~lies~~is located a few decametres below the shallow aquifer in maximum~~,~~ due to ~~lower~~ relatively low vertical pressure ~~build up~~gradients. Short and very permeable fault segments ~~may have~~or a small effective fault damage zone may result in a higher salinization potential due to a larger vertical ~~distance~~fault height affected by fluid displacement. The degree in shallow aquifer salinization thereby strongly depends on the initial salinity distribution in the investigated area and especially that in the fault. If a gradient in salinity exists or the salt-freshwater interface lies below the fluid displacement depth in the faults, freshwater salinization is considerably lower compared to scenarios with a sharp freshwater-brine interface located directly below the shallow freshwater aquifer. Moreover, it can be concluded that intermediate aquifers lying in between ~~a deep~~the storage reservoir and the shallow freshwater aquifer~~, like in a multi-barrier system~~, further diminish salinization ~~of~~in the shallow aquifer, because ~~saline fluids~~brine originating from the faults ~~are~~is partly displaced into these intermediate layers.

~~The unknown effective damage zone volume of fault zones is the greatest uncertainty in estimating the potential salinization of shallow freshwater resources. Hence, a site-specific assessment of a possible freshwater salinization requires a sensitivity analysis with varying effective damage zone volumes of the present faults. Furthermore, the injection-induced~~Lateral boundary conditions mainly influence the duration of brine displacement:

while open reservoir boundaries allow for fast pressure ~~increase generally results in a decrease in effective stresses. In this context, coupled hydro-mechanical simulations support estimating the (re-)activation potential of faults by shear- and/or tensile failure as well as fault fill property changes resulting from volumetric strain increments (Magri et al.,~~ dissipation, fluid flow persists for several hundred to a thousand years in a spatially restricted reservoir until the mass of brine displaced into the shallow aquifer corresponds to the overall injected fluid mass (assuming zero pore compressibility). Considering~~2013; Röhmann et al., 2013; Cappa and Rutqvist, 2011; Chin et al., 2000). With respect to~~ our simulation results, we conclude that hydraulically conductive fault zones do not necessarily lead to freshwater salinization owing to upward ~~fluid~~brine displacement. This principally depends on the initial salinity distribution, effective volume of the fault damage zone and the ~~geological boundary conditions. We showed that numerical simulations are applicable to obtain site-specific insights on the relevant factors affecting dynamic fluid flow processes. Since every field site is very complex and especially most of the heterogeneities in the subsurface are unknown, we focused here on selected end members to estimate the site-specific bandwidth of the potential salinization. Field explorations should be employed prior to any underground utilization to obtain more accurate data, especially on the effective damage zone volume of present fault zones as well as the initial salinity distribution.~~ hydrogeological boundary conditions.

We demonstrated how to apply numerical simulations to provide site-specific insights on the relevant factors affecting dynamic fluid flow processes and brine displacement into shallow freshwater aquifers. Since most storage sites are very complex from the geological point of view, and especially the spatial distribution of heterogeneities in the subsurface at the regional scale is not well known, we focused here on selected parameter end members to estimate the site-specific bandwidth of potential freshwater salinization. Field explorations have to be employed prior to any underground utilization to obtain the most accurate data, especially on hydraulic properties of existing fault zones as well as the initial salinity distribution.

Acknowledgements

We would like to thank our colleagues Benjamin Nakaten and Marco De Lucia (GFZ German Research Centre for Geosciences) for technical support and constructive comments.

References

Bense, V.F. and Person, M.A.: Faults as conduit-barrier systems to fluid flow in siliciclastic sedimentary aquifers, Water Resour. Res., 47 (W05421), 1-18, doi:10.1029/2005WR004480, 2006.

Bergmo, P.E.S., Grimstad, A.-A. and Lindeberg, E.: Simultaneous CO_2 injection and water production to optimise aquifer storage capacity, Int. J. Greenh. Gas Con., 5 (3), 555-564, doi:10.1016/j.ijggc.2010.09.002, 2011.

Beutler, G. and Stackebrandt, W.: Der Schollenbau des Tafeldeckgebirges von Brandenburg – Vorschlag für eine einheitliche Benennung [The tectonic pattern of the sedimentary cover of Brandenburg – suggestion for a uniform nomenclature~~,~~], Brandenburgische Geowissenschaftliche Beiträge, 19 (1), 93–109, ~~Kleinmachnow,~~ 2012~~, (in German).~~,

Birkholzer, J.T., Zhou, Q. and Tsang, C.-F.: Large-scale impact of CO_2 storage in deep saline aquifers: a sensitivity study on pressure response in stratified systems, Int. J. Greenh. Gas Con., 3, 181–194, doi:10.1016/j.ijggc.2008.08.002, 2009.

Birkholzer, J.T., Nicot, J.P., Oldenburg, C.M., Zhou, Q., Kraemer, S. and Bandilla, K.: Brine flow up a well caused by pressure perturbation from geologic carbon sequestration: static and dynamic evaluations, Int. J. Greenh. Gas Con., 5, 850–861, doi:10.1016/j.ijggc.2011.01.003, 2011.

Buscheck, T.A., Sun, Y., Hao, Y., Wolery, T.J., Bourcier, W., Tompson, A. F.B., Jones, E.D., Friedmann, S.J. and Aines R.D.: Combining brine extraction, desalination, and residual-brine reinjection with CO_2 storage in saline formations: Implications for pressure management, capacity, and risk mitigation, Energy Procedia, 4, 4283-4290 doi:10.1016/j.egypro.2011.02.378, 2011.

Caine, J., Evans, J. and Forster, C.: Fault zone architecture and permeability structure, Geology, 24 (11), 1025-1028, doi:10.1130/0091-7613(1996)024<1025:FZAAPS>2.3.CO;2, 1996.

Cappa, F. and Rutqvist, J.: Modeling of coupled deformation and permeability evolution during fault reactivation induced by deep underground injection of CO_2, Int. J. Greenh. Gas Con., 5, 336–346, doi:10.1016/j.ijggc.2010.08.005, 2011.

Formatted: German (Germany)

Formatted: German (Germany)

Formatted: German (Germany)

Formatted: German (Germany)

Formatted: German (Germany)

Formatted: German (Germany)

Cavanagh, A. and Wildgust, N.: Pressurization and brine displacement issues for deep saline formation CO_2 storage, Energy Procedia, 4, 4814–4821, doi:10.1016/j.egypro.2011.02.447, 2011.

Chin, L.Y., Raghavan, R. and Thomas, L.K.: Fully coupled geomechanics and fluid-flow analysis of wells with stress-dependent permeability, SPE J., 5 (1), 32-45, Paper 58968, doi:10.2118/58968-PA, 2000.

Chiaramonte, L., Zoback, M. D., Friedmann, S. J. and Stamp V.: Seal integrity and feasibility of CO_2 sequestration in the Teapot Dome EOR Pilot: Geomechanical site characterization, Environ. Geol., 54 (8), 1667-1675, doi:10.1007/s00254-007-0948-7, 2008.

Court, B., Bandilla, K.W., Celia, M.A., Buscheck, T.A., Nordbotten, J.M., Dobossy, M. and Janzen, A.: Initial evaluation of advantageous synergies associated with simultaneous brine production and CO_2 geological sequestration, Int. J. Greenh. Gas Con., 8, 90-100, doi:10.1016/j.ijggc.2011.12.009, 2012.

Crawford, B.R., Faulkner, D.R, and Rutter, E.H.: Strength, porosity, and permeability development during hydrostatic and shear loading of synthetic quartz-clay fault gouge, J. Geophys. Res.-Sol. Ea., 113, B03207, doi:10.1029/2006JB004634, 2008.

Dempsey, D., Kelkar, S. and Pawar, R.: Passive injection: A strategy for mitigating reservoir pressurization, induced seismicity and brine migration in geologic CO_2 storage, Int. J. Greenh. Gas Con., 28, 96-113, doi:10.1016/j.ijggc.2014.06.002, 2014.

Egholm, D.L., Clausen, O.R., Sandiford, M., Kristensen, M.B. and Korstgård, J.A.: The mechanics of clay smearing along faults, Geology, 36 (10), 787-790, doi:10.1130/G24975A.1, 2008.

Faulkner, D.R., Jackson, C.A.L., Lunn, R.J., Schlische, R.W., Shipton, Z.K., Wibberley, C.A.J. and Withjack, M.O.: A review of recent developments concerning the structure, mechanics and fluid flow properties of fault zones, J. Struct. Geol., 32, 1557–1575, doi:10.1016/j.jsg.2010.06.009, 2010.

Fisher, Q.J. and Knipe, R.J.: The permeability of faults within siliciclastic petroleum reservoirs of the North Sea and Norwegian Continental Shelf, Mar. Petrol. Geol., 18 (10), 1063-1081, doi:10.1016/S0264-8172(01)00042-3, 2001.

Forster, C.B. and Evans, J.P.: Fluid flow in thrust faults and crystalline thrust sheets: Results of combined field and modeling studies, Geophys. Res. Lett., 18, 979-982, 1991.

Grube, A., Wichmann, K., Hahn, J. and Nachtigall, K.: Geogene Grundwasserversalzung in den Poren-Grundwasserleitern Norddeutschlands und ihre Bedeutung für die Wasserwirtschaft, DVGW-Technologiezentrum Wasser, Band 9, Karlsruhe, 2000~~, (in German).~~.

Hannemann, M. and Schirrmeister, W.: Paläohydrogeologische Grundlagen der Entwicklung der Süß-/Salzwassergrenze und der Salzwasseraustritte in Brandenburg [Paleohydrological basics of the development of the boundary of fresh and salt water as well as of the salt water-outlets in Brandenburg~~,~~], Brandenburgische Geowissenschaftliche Beiträge, 5 (1), 61-72, ~~Kleinmachnow,~~ 1998~~, (in German).~~.

~~Hotzan, G. and Voss, T.:~~ Harris, S.D, McAllister, E., Knipe, R.J. and Odling, N.E.: Predicting the three-dimensional population characteristics of fault zones: a study using stochastic models, J. Struct. Geol., 25 (8), 1281-1299, doi:10.1016/S0191-8141(02)00158-X, 2003.

Hotzan, G. and Voss, T.: Komplexe hydrogeochemisch-genetische Kartierung zur Einschätzung der Salzwassergefährdung pleistozäner und tertiärer Grundwasserleiter im Raum Storkow-Frankfurt (Oder)-Eisenhüttenstadt [Complex hydrogeochemic-genetic mapping for evaluation of the endangerment of pleistocene and tertiary aquifers by saline waters in the region Storkow-Frankfurt (Oder)-Eisenhüttenstadt~~,~~], Brandenburgische Geowissenschaftliche Beiträge, 20 (1/2), 62-82, ~~Kleinmachnow,~~ 2013~~, (in German).~~.

IEA Greenhouse Gas R&D Programme (IEA GHG): CCS Site Characterization Criteria, Technical Study, Report No. 2009/10, 130 pp. 2008.

IPCC - Metz, B., Davidson, O., de Coninck, H.C., Loos, M. and Meyer L.A. (Eds.): IPCC Special Report on Carbon Dioxide Capture and Storage, Prepared by Working Group III of the Intergovernmental Panel on Climate Change, Cambridge University Press, New York, ~~pp.~~ 431~~,~~ pp., 2005.

Jourde, H., Flodin, E., Aydin, A., Durlovsky, L. and Wen, X.: Computing permeability of fault zones in eolian sandstone from outcrop measurements, AAPG Bull., 86 (7), 1187-1200, doi:10.1306/61EEDC4C-173E-11D7-8645000102C1865D, 2002.

Formatted: German (Germany)
Formatted: German (Germany)
Formatted: German (Germany)
Formatted: German (Germany)
Formatted: German (Germany)
Formatted: German (Germany)
Formatted: German (Germany)
Formatted: German (Germany)
Formatted: Space After: 12 pt

Kempka, T., Nielsen, C.M., Frykman, P., Shi, J.-Q., Bacci, G. and Dalhoff, F.: Coupled Hydro-Mechanical Simulations of CO_2 Storage Supported by Pressure Management Demonstrate Synergy Benefits from Simultaneous Formation Fluid Extraction, Oil Gas Sci. Technol., 70 (4), 599-613, doi:10.2516/ogst/2014029, 2015.

Kempka, T., Herd, R., Huenges, E., Endler, R., Jahnke, C., Janetz, S., Jolie, E., Kühn, M., Magri, F., Meinert, P., Moeck, I., Möller, M., Muñoz, G., Ritter, O., Schafrik, W., Schmidt-Hattenberger, C., Tillner, E., Voigt, H.-J. and Zimmermann, G.: Joint Research Project Brine: Carbon Dioxide Storage in Eastern Brandenburg: Implications for Synergetic Geothermal Heat Recovery and Conceptualization of an Early Warning System Against Freshwater Salinization. In: Liebscher, A. and Münch, U. (Eds.), Geological Storage of CO_2 – Long Term Security Aspects. GEOTECHNOLOGIEN Science Report No.22, Advanced Technologies in Earth Sciences, Springer International Publishing, ~~p.~~ 139-166, 2015.

~~Kühn, M., Kempka, T. and Jolie, E.: Evaluation of potential pressurisation and salinisation of freshwater reservoirs by brine migration as a result of geological CO_2 storage, 4th International Conference GeoProc2011, Perth, Australia, 6-9 July 2011, 2011.~~

Kempka, T., Klapperer, S. and Norden, B.: Coupled hydro-mechanical simulations demonstrate system integrity at the Ketzin pilot site for CO_2 storage. In: Alejano, L., Perucho, A., Olalla, C. and Jiménez, R. (Eds.), Rock Engineering and Rock Mechanics: Structures in and on Rock Masses; Proceedings of EUROCK 2014, ISRM European Regional Symposium, Leiden: CRC Press/Balkema, 1317-1322, 2014.

Kühn, M. and Kempka, T.: CO_2 Pressurisation of a Storage Reservoir does not Lead to Salinization of Shallower Aquifers through Intact Caprocks, Energy Procedia, 76, 607-615, doi:10.1016/j.egypro.2015.07.880, 2015.

Magri, F., Tillner, E., Wang, W., Watanabe, N., Zimmermann, G. and Kempka, T.: 3D Hydro-mechanical Scenario Analysis to Evaluate Changes of the Recent Stress Field as a Result of Geological CO_2 Storage, Energy Procedia 40, 375-383, doi:-10.1016/j.egypro.2013.08.043, 2013.

Mitchell, T. and Faulkner, D.: The nature and origin of off-fault damage surrounding strike-slip fault zones with a wide range of displacements: A field study from the Atacama fault system, northern Chile, J. Struct. Geol., 31 (8), 802-816, doi:10.1016/j.jsg.2009.05.002,- 2009.

Formatted: Font color: Black

Formatted: English (U.S.)

Nakaten, B., Tillner, E. and Kempka, T.: Virtual Elements for Representation of Faults, Cracks and Hydraulic Fractures in Dynamic Flow Simulations, Energy Procedia, 40, 447-453, doi:10.1016/j.egypro.2013.08.051, 2013.

Nicot, J.: Evaluation of large-scale CO_2 storage on fresh-water sections of aquifers: An example from the Texas Gulf Coast Basin, Int. J. Greenh. Gas Con., 2 (4), 582-593, doi:10.1016/j.ijggc.2008.03.004, 2008.

Nordbotten, J. M., Celia, M. A. and Bachu, S.: Analytical solutions for leakage rates through abandoned wells, Water Resour. Res., 40, W04204, doi:10.1029/2003WR002997, 2004.

Person, M., Banerjee, A., Rupp, J., Medina, C., Lichtner, P., Gable, C., Pawar, R., Celia, M., McIntosh, J. and Bense, V.: Assessment of basin-scale hydrologic impacts of CO_2 sequestration, Illinois basin, Int. J. Greenh. Gas Con., 4 (5), 840-854, doi:10.1016/j.ijggc.2010.04.004, 2010.

Odling, N.E., Harris, S.D. and Knipe, R.J.: Permeability scaling properties of fault damage zones in siliclastic rocks, J. Struct. Geol., 26 (9), 1727-1747, doi:10.1016/j.jsg.2004.02.005, 2004.

Oldenburg, C.M. and Rinaldi, A.P.: Buoyancy Effects on Upward Brine Displacement caused by CO_2 Injection, Transport Porous. Med., 87 (2), 525-550, doi:10.1007/s11242-010-9699-0, 2011.

Pruess, K.: ECO2N: A TOUGH2 Fluid Property Module for Mixtures of Water, NaCl, and CO_2, Lawrence Berkeley National Laboratory, Berkeley, CA, 66 pp., 2005.

Rinaldi, A.P., Vilarrasa, V., Rutqvist, J. and Cappa, F.: Fault reactivation during CO_2 sequestration: effects of well orientation on seismicity and leakage. Greenhouse Gases: Science and Technology, 5 (5), 645-656, doi:10.1002/ghg.1511, 2015.

Röhmann, L., Tillner, E., Magri, F., Kühn, M. and Kempka, T.: Fault Reactivation and Ground Surface Uplift Assessment at a Prospective German CO_2 Storage Site. Energy Procedia 40, 437-446., doi:-10.1016/j.egypro.2013.08.050, 2013.

Schlumberger: Petrel Seismic-to-Evaluation Software, Version 2011.2.7, 2011.

Formatted: Don't adjust space between Latin and Asian text, Don't adjust space between Asian text and numbers

Formatted: Font color: Auto

Shipton, Z.K. and Cowie, P.A.: A conceptual model for the origin of fault damage zone structures in high-porosity sandstone, J. Struct. Geol., 25, 333-344, doi:10.1016/S0191-8141(02)00037-8, 2003.

Shipton, Z.K., Soden, A., Kirkpatrick, J., Bright, A. and Lunn, R.: How Thick is a Fault? Fault Displacement-Thickness Scaling Revisited~~, in:~~. In: Abercrombie, R., McGarr, A., Di Toro, G., Kanamori, H. (Eds.), Earthquakes: Radiated Energy and the Physics of Faulting, American Geophysical Union, Washington DC, 193-198, doi:10.1029/170GM19, 2006.

Span, R. and Wagner, W.: A New Equation of State for Carbon Dioxide Covering the Fluid Region from the Triple-Point Temperature to 1100 K at Pressures up to 800 MPa, J. Phys. Chem. Ref. Data, 25 (6), 1509-1596, doi:10.1063/1.555991, 1996.

Stackebrandt, W.: Grundzüge des geologischen Baus von Brandenburg [Outline of the geological setting of Brandenburg~~,~~], Brandenburgische Geowissenschaftliche Beiträge, 5 (2), 3~~–~~7,~~ Kleinmachnow, 2010, (in German).~~ 1998.

Tesch, J.~~: Hydrogeological Report with groundwater reserve estimation, VE 1987 – VED.~~, Burmann, G., Schwamm, G. and Nillert, P.: Hydrogeologischer Ergebnisbericht mit Grundwasservorratsberechnung, Vorerkundung Fürstenwalde, VEB Hydrogeologie Nordhausen, BT Berlin, 1-309, Berlin, 1987~~. (in German,~~ (unpublished~~)~~).

Tillner, E., Shi, J.-Q., Bacci, G., Nielsen, C.M., Frykman, P., Dalhoff, F. and Kempka, T.: Coupled Dynamic Flow and Geomechanical Simulations for an Integrated Assessment of CO_2 Storage Impacts in a Saline Aquifer, Energy Procedia, 63, 2879-2893, doi:10.1016/j.egypro.2014.11.311, 2014.

Tillner, E., Kempka, T., Nakaten, B. and Kühn, M.: Geological CO_2 Storage Supports Geothermal Energy Exploitation: 3D Numerical Models Emphasize Feasibility of Synergetic Use, Energy Procedia, 37, 6604-6616, doi:10.1016/j.egypro.2013.06.593, 2013.

Tillner, E., Kempka, T., Nakaten, B. and Kühn, M.: Brine migration through fault zones: 3D numerical simulations for a prospective CO_2 storage site in Northeast Germany, Int. J. Greenh. Gas Con., 19, 689-703, doi:10.1016/j.ijggc.2013.03.012, 2013.

Trinkwasserverordnung – TrinkwV 2001: Verordnung über die Qualität von Wasser für den menschlichen Gebrauch vom 21.05.2001 (BGBl. I S. 959). Trinkwasserverordnung in der

Formatted: Font color: Black

Formatted: German (Germany)

Formatted: German (Germany)

Formatted: German (Germany)

Formatted: German (Germany)

Formatted: German (Germany)

Formatted: German (Germany)

Formatted: German (Germany)

Fassung der Bekanntmachung vom 2. August 2013 (BGBl. I S. 2977), die durch Artikel 4 Absatz 22 des Gesetzes vom 7. August 2013 (BGBl. I S. 3154) geändert worden ist.

Vattenfall: Antrag auf Erteilung einer Erlaubnis zur Aufsuchung bergfreier Bodenschätze zu gewerblichen Zwecken, http://www.lbgr.brandenburg.de/media_fast/4055/Antrag%200_Aufsuchung%20bergfreier%20Bodensch%C3%A4tze_Bkh_20090306.15564291.pdf, 12 pp., last access: 18 December 2014, 2009~~, (in German).~~.

Vattenfall: Hauptbetriebsplan – Aufsuchungsarbeiten in Bezug auf den bergfreien Bodenschatz Sole im Erlaubnisfeld Birkholz-Beeskow, 28 pp., http://www.lbgr.brandenburg.de/media_fast/4055/Bkh_HBP_Finale.pdf, last access: 18 December 2014, 2010~~ (in German).~~.

Vilarrasa, V. and Carrera, J.: Geologic carbon storage is unlikely to trigger large earthquakes and reactivate faults through which CO_2 could leak. Proc. Nat. Acad. Sci. USA, 112 (19), 5938-5943, doi:10.1073/pnas.1413284112, 2015.

Walter, L., Binning, P.J., Oladyshkin, S., Flemisch, B. and Class, H.: Brine migration resulting from CO_2 injection into saline aquifers – An approach to risk estimation including various levels of uncertainty, Int. J. Greenh. Gas Con., 9, 495-506, doi:10.1016/j.ijggc.2012.05.004, 2012.

Wibberley, C. A. J., Yielding, G. and Toro, G.: Recent advances in the understanding of fault zone internal structure: a review~~, in:~~. In: Wibberley, C.A.J., Kurz, W., Imber, J., Holdsworth, R.E., Collettini, C. (Eds.), The Internal Structure of Fault Zones: Implications for Mechanical and Fluid-Flow Properties, Geological Society of London, 5~~–~~33, doi: 10.1144/SP299.2, 2008.

Yamamoto, H., Zhang, K., Karasakib, K., Marui, A., Hitoshi Uehara, H. and Nishikawa, N.: Numerical investigation concerning the impact of CO_2 geologic storage on regional groundwater flow, Int. J. Greenh. Gas Con., 3 (5), 586-599, doi:10.1016/j.ijggc.2009.04.007, 2009.

Zeidouni, M.: Analytical model of leakage through fault to overlying formations, Water Resour. Res., 48, W00N02, 1-17, doi:10.1029/2012WR012582, 2012.

Formatted: Font color: Black

Zhang, K., Wu, Y.S. and Pruess, K.: User's Guide for TOUGH2-MP – A Massively Parallel Version of the TOUGH2 Code, Earth Sciences Division, Lawrence Berkeley National Laboratory, Berkeley, 108 pp., 2008.

Zhou, Q., Birkholzer, J., Mehnert, E., Lin, Y. and Zhang, K.: Modelling Basin- and Plume-Scale Processes of CO_2 Storage for Full-Scale Deployment, Ground Water, 48 (4), 494-514, doi:10.1111/j.1745-6584.2009.00657.x, 2010.

1 Table 1. Summary of numerical simulations of brine migration resulting from CO_2 injection

Authors	Study area and model extend	Reservoir boundaries	Simulator	Injection ~~rate of CO_2~~ and duration	Injected fluid	Objectives	Results
Birkholzer et al., 2009	• synthetic • 125 000 km² (radial symmetric)	open	TOUGH2/ ECO2N	1.52 Mt yr^{-1} over 30 years	CO_2	Pressure build-up and brine migration in the reservoir and through low permeable caprocks	• Considerable pressure build-up in a distance of > 100 km from injection zone • Vertical brine migration through a sequence of seals extremely unlikely
Birkholzer et al., 2011	• synthetic • 12 km² (radial symmetric)	closed	TOUGH2/ EOS7	Simulated by pressure build-up	-	Brine migration up a leaking wellbore	• Continuous flow only occurs if pressure perturbation in the reservoir is large enough to overcome the increased weight of the fluid column
Nicot, 2008	• Gulf Coast, USA • 80 000 km²	closed	MODLFLOW96	50 Mt yr^{-1} and 250 Mt yr^{-1} over 50 years	Water	Pressure build-up and brine migration ~~of brine~~ in the reservoir and through low permeable caprocks	• Average water table rise is in the same order of magnitude as seasonal and inter-annual variations
Oldenburg and Rinaldi, 2011	• synthetic • 1 km (2D)	closed	TOUGH2/ EOS7	Simulated by pressure build-up	-	Brine displacement in shallower aquifers through a vertical conduit (borehole or fault)	• Depending on brine density and pressure gradient fluid migrates upward until a new static steady-state equilibrium is reached or a sustained flow develops, if the brine is allowed to spread laterally.
Person et al., 2010	• Illinois basin, USA • 3 000 km² - 241 000 km²	closed and open	Analytical single phase and sharp-interface models	80 Mt yr^{-1} over 100 years		Pressure build-up and CO_2/brine migration in the reservoir and through low permeable caprocks	• No significant lateral brine migration due to distributed injection and vertical brine leakage across the confining unit • Pressure propagation (> 0.3 bar) up to a distance of 10-25 km away from the injection wells
Tillner et al., 2013	• North German Basin • 1 764 km²	closed and open	TOUGH2-MP/ ECO2N	1.7 Mt yr^{-1} over 20 years	CO_2	Brine migration through faults dependent on reservoir compartmentalisation and fault permeability	• Degree of pressurization is the driving mechanism for brine migration • Permeability of fault zones does not influence salinization of shallower aquifers significantly
Yamamoto et al., 2009	• Bay of Tokyo, Japan • 4 200 km²	open	TOUGH2-MP/ ECO2N	10 Mt yr^{-1} over 100 years	CO_2	Pressure build-up and brine migration in the reservoir and through low permeable caprocks	• Pressure build-up of a few bars can occur in the shallow confined aquifers over extensive regions

Authors	Study area and model extend	Reservoir boundaries	Simulator	Injection ~~rate of CO_2~~ and duration	Injected fluid	Objectives	Results
Zhou et al., 2010	• Illinois basin, USA • 241 000 km²	open	TOUGH2 - ECO2N	100 Mt yr^{-1} over 50 years	CO_2	Pressure build-up and CO_2/brine migration in the reservoir and through low permeable caprocks	• Pressure build-up of 1 bar and 0.1 bar can be expected as far as 150 km and 300 km from the injection area, respectively • pressure increase of 35 bar at injection does not affect caprock integrity
This study	• North German Basin • 10 000 km²	closed and open	TOUGH2-MP/ ECO2N	1.7 Mt yr^{-1} over 20 years	Water	Brine migration through fault zones depending on different geological conditions	• Boundary conditions, fault length and existence of an overlying secondary reservoir affect pressure development in the reservoir and thereby freshwater salinization

Table 2. Vertical grid discretization, depth and hydraulic parameters for the active geological units.

Unit	k (mD)	Φ (%)	thickness (m)	depth (m)	element layers	vertical resolution (m)
Rupelian basal sands	1 000	20	20	-110 to -130	2	10
Muschelkalk Formation	200	20	140	-1 025 to -1 165	7	19.9
Detfurth Formation	400	17	23	-1 425 to -1 448	2	11.5
Faults	700	18.5			50	19.9

Table 3. Overview about all calculated scenarios~~, their mean reservoir pressures~~ assuming a fault permeability of 700 mD. Maximum pressure increase at the ~~end of injection as well as depth~~base of ~~origin~~Fault 1 and ~~distribution~~displacement depths in Fault 1 are observed at the central part of the ~~brine displaced into the shallow aquifer.~~fault.

Scenario	Fault length (km)	Effective damage zone volume (m^3)	Δp at base of Fault 1 (bar) [a]	Maximum displacement depth in Fault 1 (m) [ab]	Rupelian basal sand			Duration of mass flow (yrs) [d]
					Relative salt mass change (kg)[a]	Salinization area (m^2) [ac]	Average salt mass in salinization area (kg m^{-2}) [a]	
$F_1^{2km}\ B_C$	2	1.8×10^8	19.0	131.7	6.17×10^9	1.98×10^7	311.6	330
$F_1^{2km}\ B_O$			12.4	105.4	4.86×10^9	1.64×10^7	296.3	31
$F_1^{2km}\ B_C\ SR_{200mD}$			9.0	69.5	2.93×10^9	1.41×10^7	207.8	1050
$F_1^{2km}\ B_O\ SR_{200mD}$			6.1	56.3	2.34×10^9	1.24×10^7	188.7	31
$F_1^{2km}\ B_C^*$			18.9	131.7	5.80×10^8	2.11×10^7	27.5	275
$F_1^{60km}\ B_C$	60	4.9×10^9	12.1	29.8	1.08×10^{10}	7.65×10^7	141.2	115
$F_1^{60km}\ B_O$			9.7	28.4	8.45×10^9	6.73×10^7	125.6	31
$F_1^{60km}\ B_C\ SR_{200mD}$			6.8	17.0	5.36×10^9	5.89×10^7	91.0	390
$F_1^{60km}\ B_O\ SR_{200mD}$			5.3	16.3	4.16×10^9	5.09×10^7	81.7	40
$F_{1\text{-}4}^{193km}\ B_C$	193	1.6×10^{10}	11.0	28.6	1.23×10^{10}	1.46×10^8	84.2	66
$F_{1\text{-}4}^{193km}\ B_O$			9.6	28.0	9.46×10^9	1.21×10^8	78.2	42
$F_{1\text{-}4}^{193km}\ B_C\ SR_{200mD}$			6.4	16.5	6.64×10^9	1.14×10^8	58.2	225
$F_{1\text{-}4}^{193km}\ B_O\ SR_{200mD}$			5.3	16.1	4.59×10^9	9.01×10^7	50.9	45
$F_{1\text{-}4}^{193km}\ B_O\ SR_{2000mD}$			1.2	4.0	1.06×10^9	6.03×10^7	17.6	23
$F_1^{2km}\ B_C^*$			10.9	28.6	1.67×10^8	1.66×10^7	10.1	66

[a] *t = 20 years*

[b] *counting from the base of the Rupelian basal sand*

[c] *salt concentration > 0.5 g kg^{-1} solution*

[d] *mass flow into the Rupelian basal sand > 0.1 kg s^{-1}*

[*] *Salinity gradient of 0.23 g kg^{-1} solution per meter*

Table 4. Overview about six scenarios assuming a sharp salt-/freshwater interface below the base of the Rupelian basal sand and a fault permeability of 10 mD, 200 mD and 700 mD, respectively. Maximum pressure increase at the base of Fault 1 and displacement depths in Fault 1 are again observed at the central part of the fault.

Scenario	Fault permeability (mD)	Δp at base of Fault 1 (bar) [b]	Maximum displacement depth in fault (m) [ab]	Rupelian basal sand			Duration of mass flow (yrs) [d]
				Relative salt mass change (kg) [ab]	Salinization area (m^2) [ac]	Average salt mass in salinization area (kg m^{-2}) [a]	
$F_{1\text{-}4}^{193km}\ B_C\ SR_{200mD}$	10	12.1	9.1	5.15×10^9	1.02×10^8	50.6	310
	200	7.0	17.9	6.50×10^9	1.11×10^8	58.6	270
	700	6.4	16.5	6.64×10^9	1.14×10^8	58.2	225
$F_{1\text{-}4}^{193km}\ B_O\ SR_{200mD}$	10	10.9	8.7	3.66×10^9	8.91×10^7	41.1	46
	200	5.9	17.6	4.52×10^9	8.58×10^7	52.7	45
	700	5.3	16.1	4.59×10^9	9.01×10^7	50.9	45

[a] *t = 20 years*

[b] *counting from the base of the Rupelian basal sand*

[c] *salt concentration > 0.5 g kg^{-1} solution*

[d] *mass flow into the Rupelian basal sand > 0.1 kg s^{-1}*

Formatted: Left: 3.5 cm, Right: 2 cm, Top: 2.5 cm, Bottom: 2.5 cm, Width: 29.7 cm, Height: 21 cm

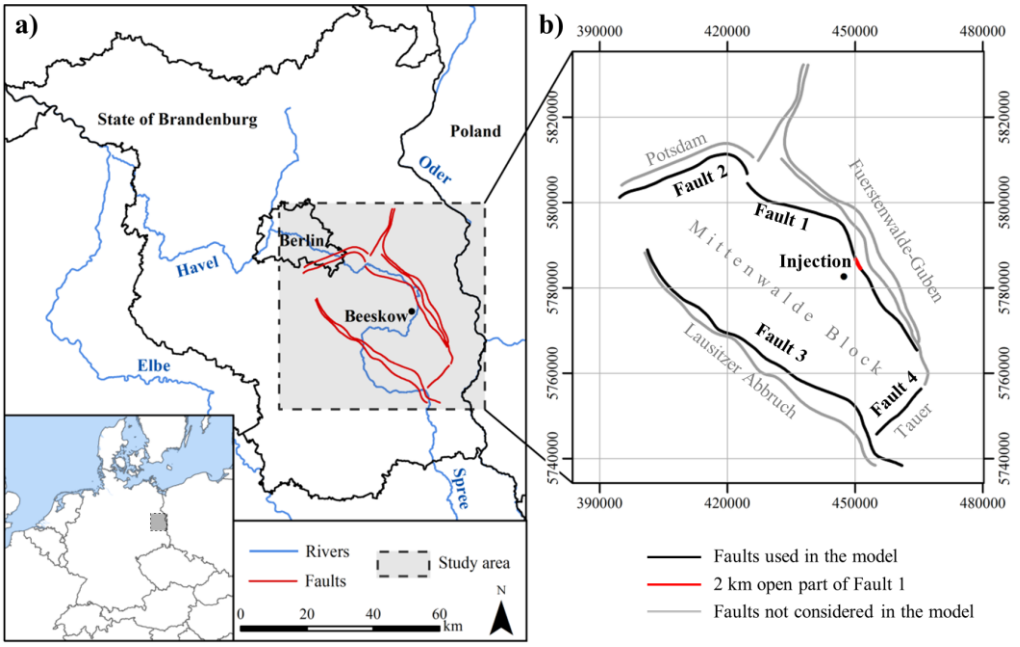

Figure 1. (a) Dashed rectangle indicates the location of the study area in the State of Brandenburg (Germany), while red lines illustrate the present fault systems. (b) Only the inner faults (black lines), facing to the injection well, were implemented to represent the entire fault zone. Axes show UTM-coordinates (WGS84/UTM zone 33N). Rivers and the outline of the states of Brandenburg and Berlin were derived from Tillner et al. (2013).

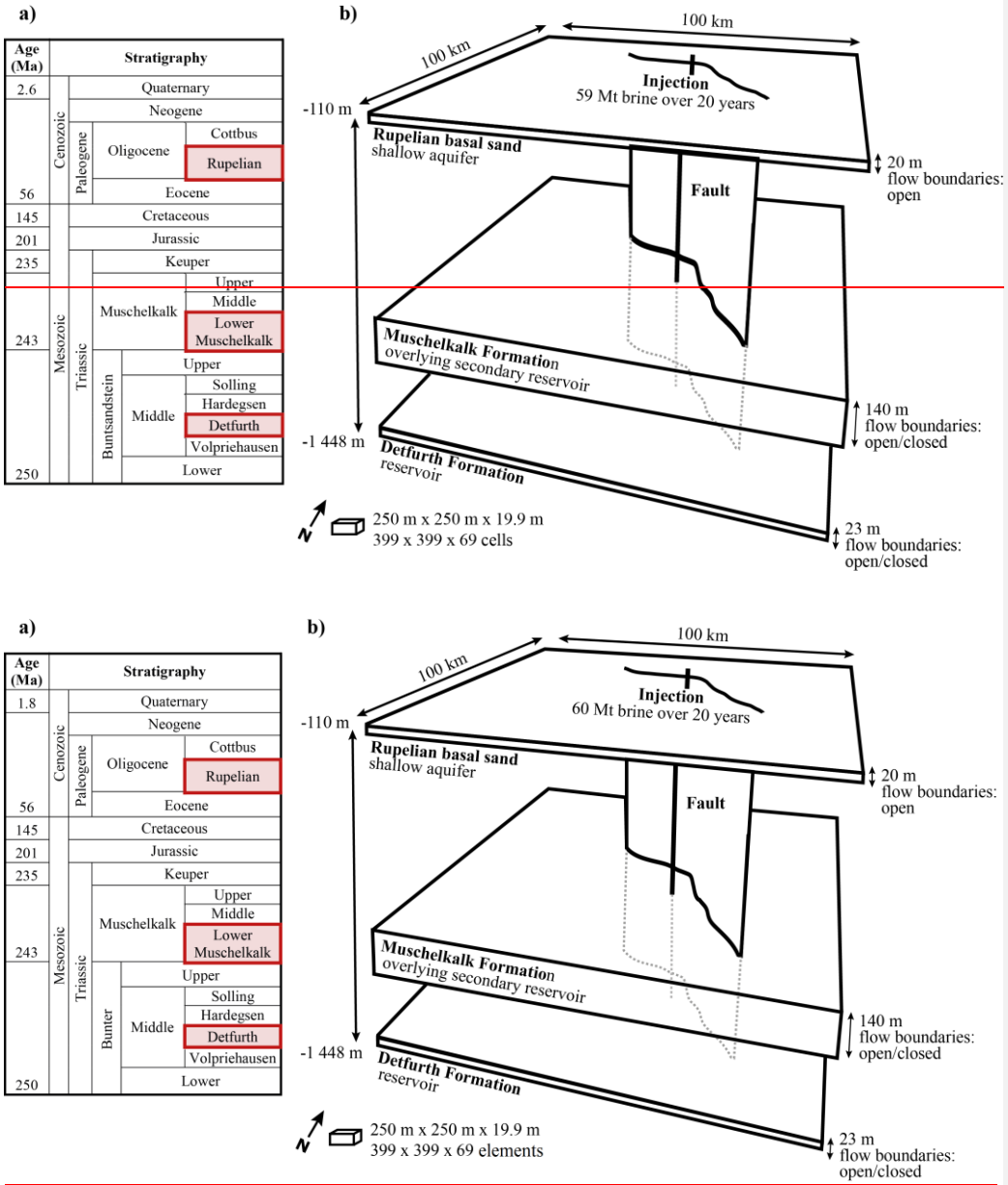

Figure 2. (a) Stratigraphy of the study area with the active model layers highlighted in red. (b) The geological 3D model with simplified topography comprises up to three layers.

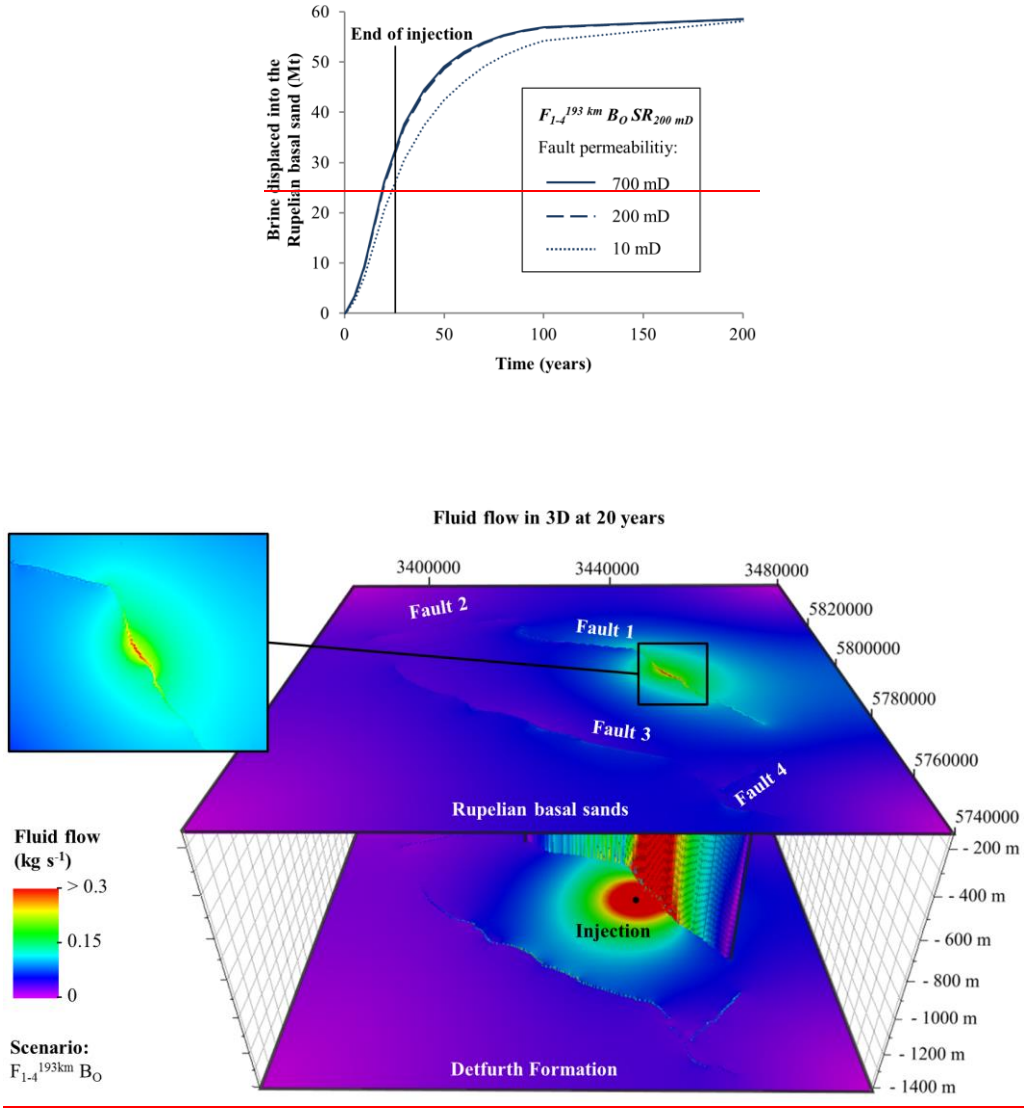

Figure 3. ~~Temporal evolution of brine displacement into the Rupelian basal sands, when all four faults are open, a secondary overlying reservoir exists and reservoir boundaries are closed. The brine mass displaced into the shallow aquifer is equal for~~In all scenarios ~~after 200 years, irrespective whether the fault permeability is higher (solid line), equal (dashed line) or lower (dotted line) to the permeability of the secondary reservoir. Lower fault permeabilities lead to retardation in mass flow only.~~

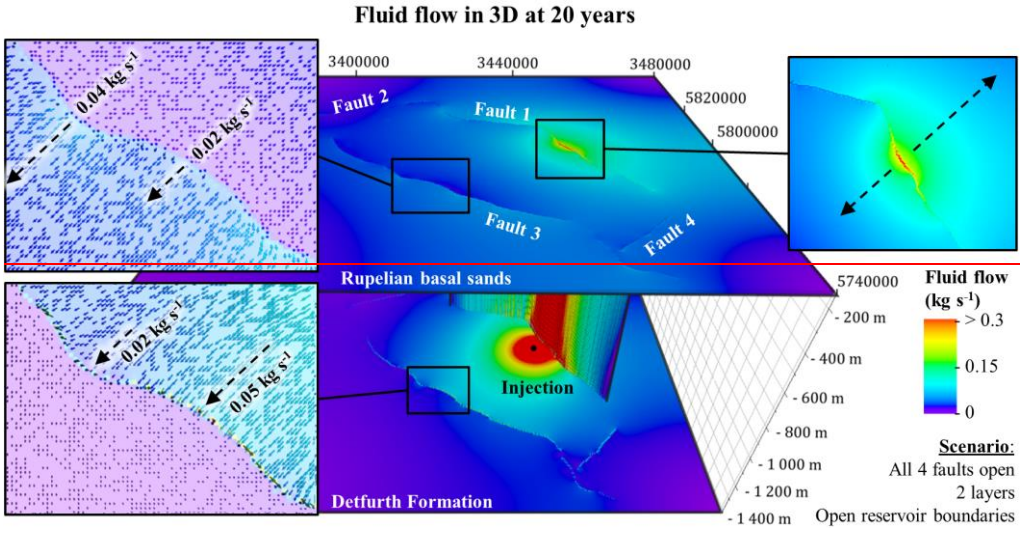

Figure 4. An injection related pattern in fluid flow, as illustrated for Scenario ~~F_{1-4}^{193km} B_O,~~ is ~~observed in all simulations. Within the reservoir, brine is displaced~~, brine is displaced radially within the reservoir and predominantly into parts of the faults lying closer to the injection well~~. It is the opposite in the shallow aquifer, where flow out of the fault is greater into parts not facing towards the injection~~ as illustrated for Scenario F_{1-4}^{193km} B_O.

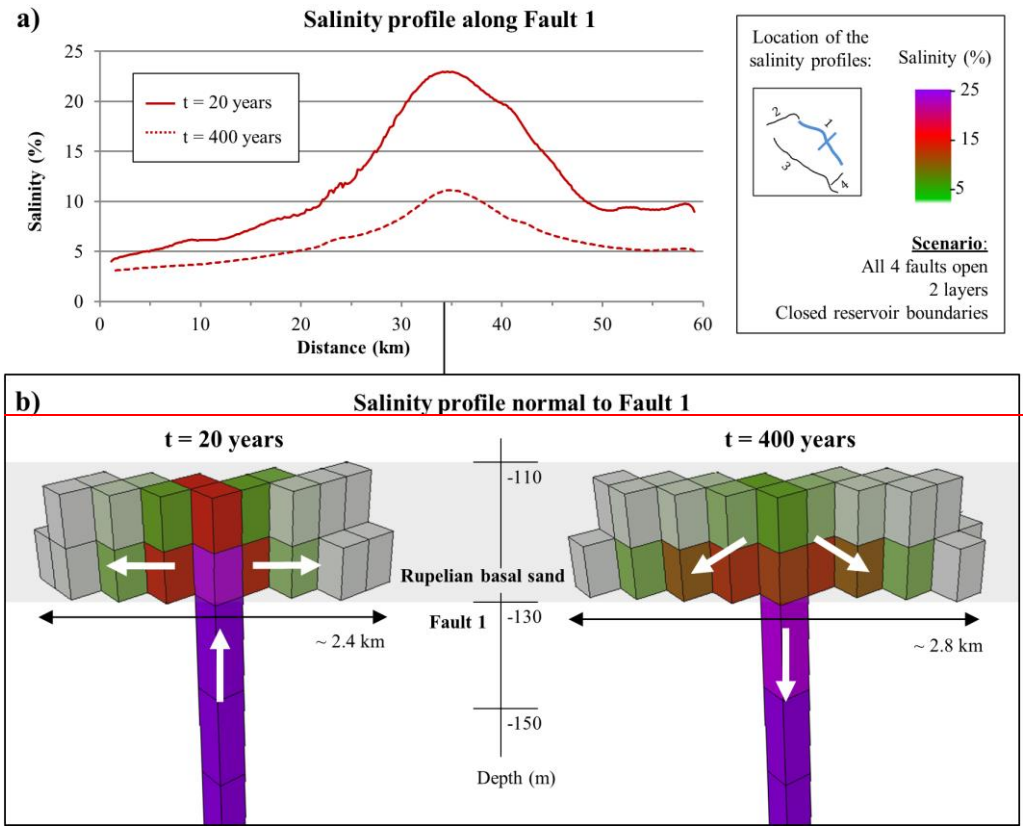
a)
Salinity profile along Fault 1
Salinity (%)
Distance (km)
t = 20 years
t = 400 years
Location of the salinity profiles:
Salinity (%)
25
15
5
Scenario:
All 4 faults open
2 layers
Closed reservoir boundaries
b)
Salinity profile normal to Fault 1
t = 20 years
t = 400 years
-110
Rupelian basal sand
Fault 1
-130
-150
~ 2.4 km
~ 2.8 km
Depth (m)

1

2

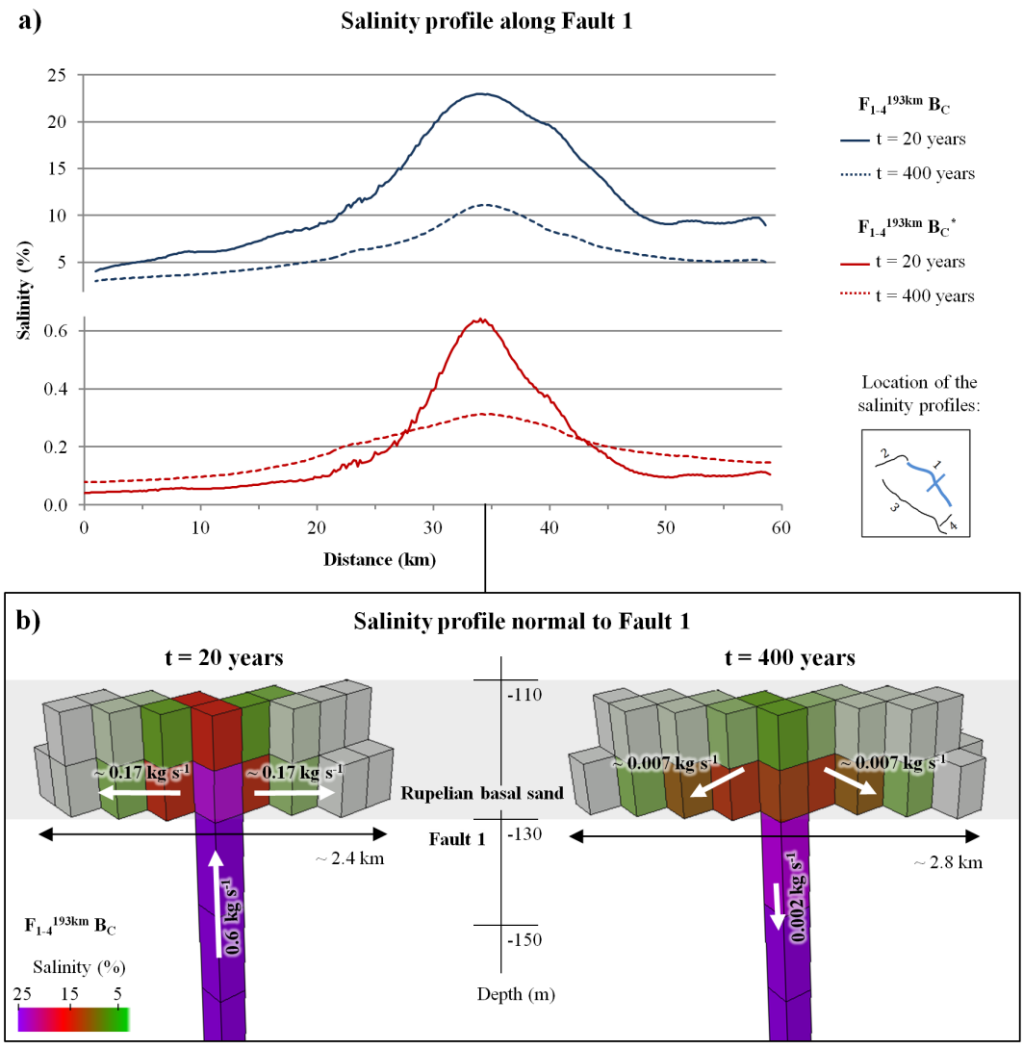

Figure ~~5~~4. (a) Profile along Fault 1 ~~(F_{1-4}^{193km} B_C)~~ shows highest salinities in the central part of the fault near to the injection well. Maximum salinities are significantly lower, if a salinity gradient is assumed (solid red line; Scenario F_{1-4}^{193km} B_C^*). A decrease in salinization due to a downward flow is observed for the time after the injection period~~.~~ and under the assumption of a sharp salt-/freshwater interface (dashed blue line; Scenario F_{1-4}^{193km} B_C). (b) Cross section normal to Fault 1 illustrates the propagation of the saltwater plume (salinities > 0.05 %), while higher salinities can be observed within the lower element layer. White arrows illustrate schematically the direction of the fluid flow at 20 years and 400 years.

1

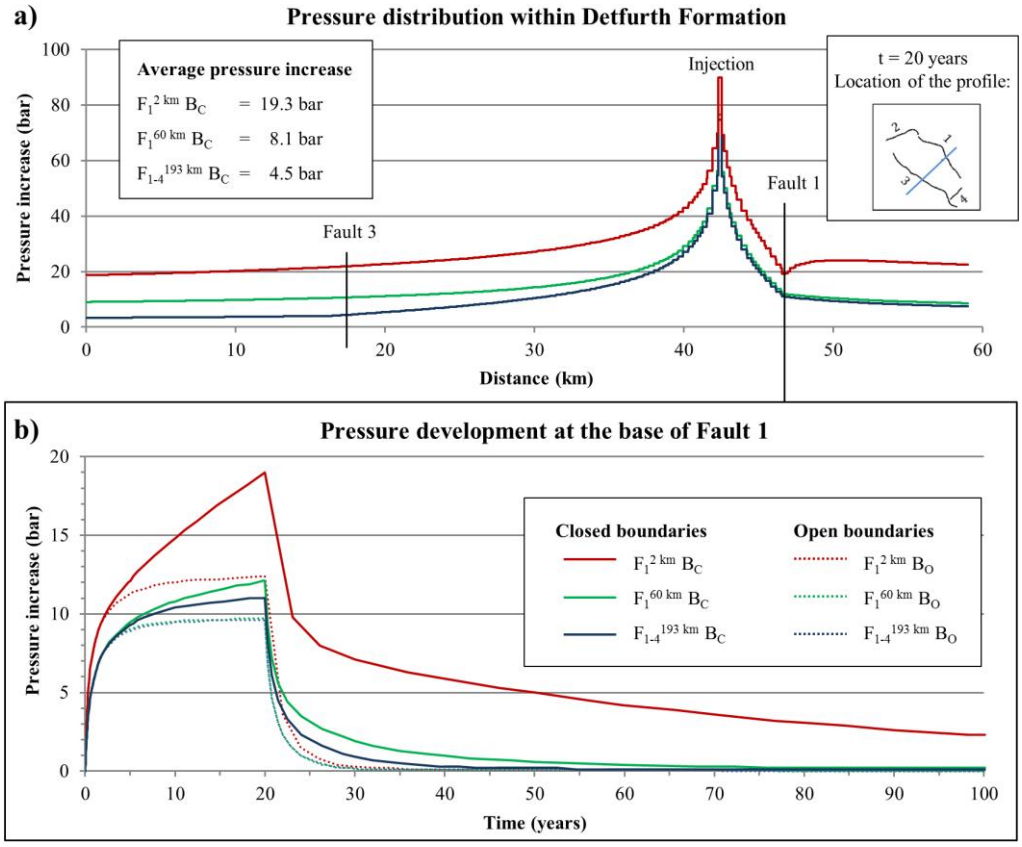

Figure ~~6~~5. (a) Distribution of the pressure increase within the Detfurth Formation along the highlighted cross section significantly varies depending on the open fault length. Highest pressurization is observed for a short fault (F_1^{2km} B_C). (b) Pressure development at the base of Fault 1 indicates a substantially faster pressure reduction for greater fault lengths.

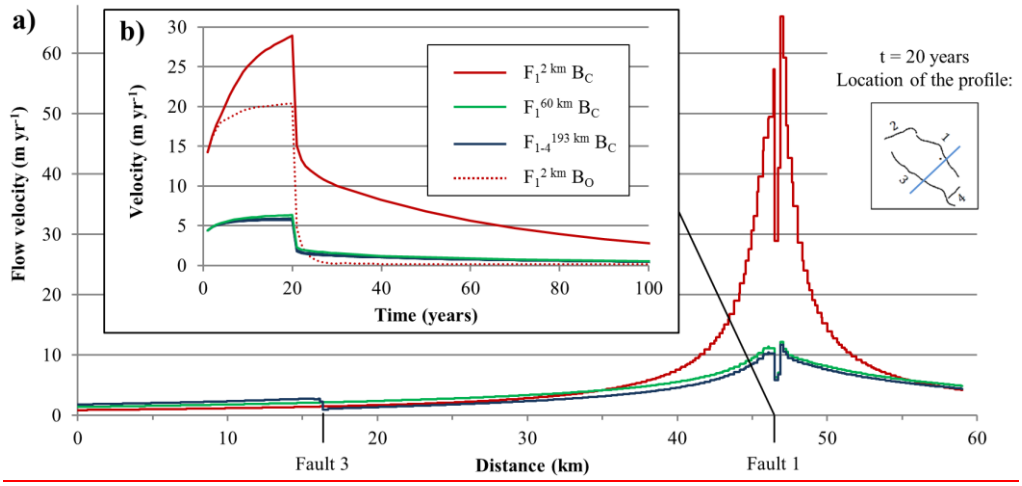

Figure 6. (a) Velocity profile within the lower element layer of the Rupelian basal sand shows highest flow velocities out of Fault 1 at the end of injection period. (b) Flow velocities out of Fault 1 increase until the end of the injection period (20 years) and decrease afterwards depending on pressure reduction of the respective scenarios.

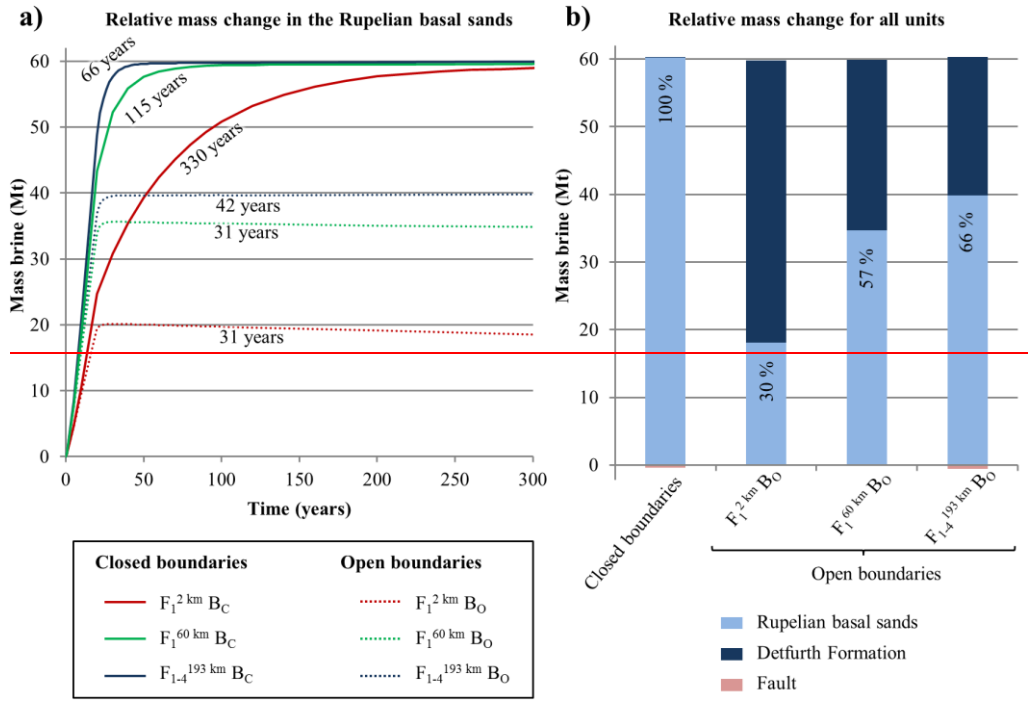
a)
Relative mass change in the Rupelian basal sands
Mass brine (Mt)
Time (years)
66 years
115 years
330 years
42 years
31 years
31 years
Closed boundaries
Open boundaries
b)
Relative mass change for all units
Mass brine (Mt)
100 %
30 %
57 %
66 %
Closed boundaries
Open boundaries
Rupelian basal sands
Detfurth Formation
Fault

1

2

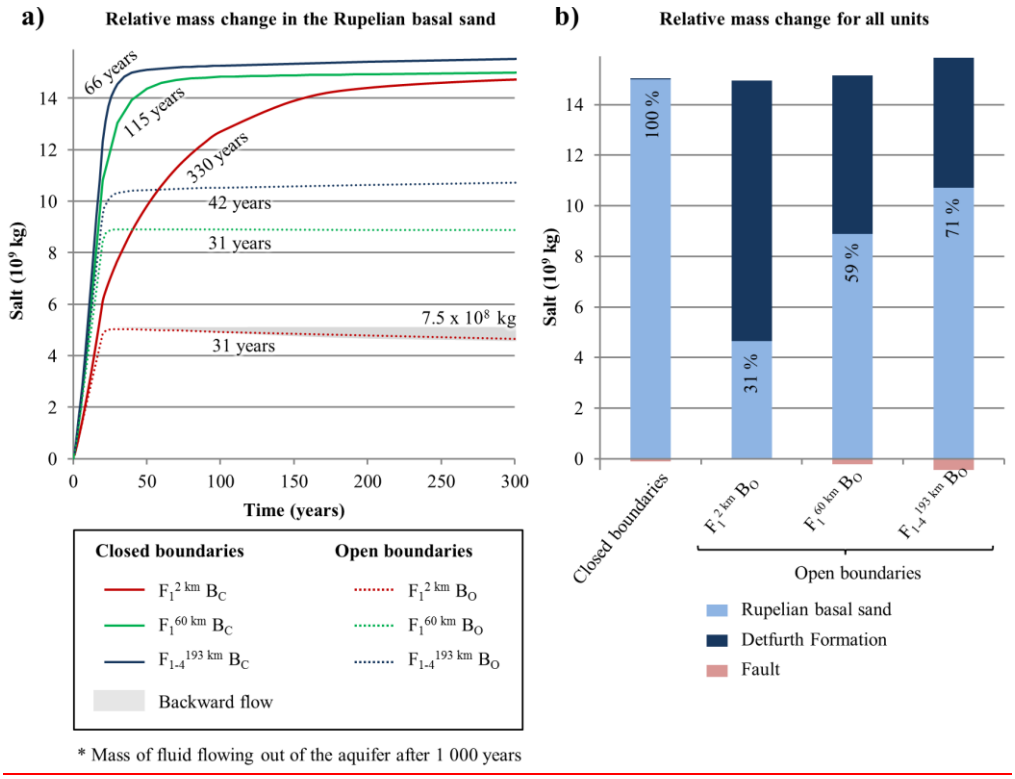

Figure 7. (a) Relative salt mass change in the Rupelian basal ~~sands~~sand shows that the mass of ~~brine~~salt displaced into the shallow aquifer corresponds to the overall injected fluid mass, if reservoir boundaries are closed. As indicated by the duration of mass flow (black numbers), only a temporal effect on fluid migration occurs. (b) Relative mass change for all lithological units after ~~330 years (mass flow < 0.1 kg s^{-1} for all scenarios)~~20 years illustrates a considerably reduced salinization of the Rupelian basal ~~sands~~sand for open reservoir boundaries.

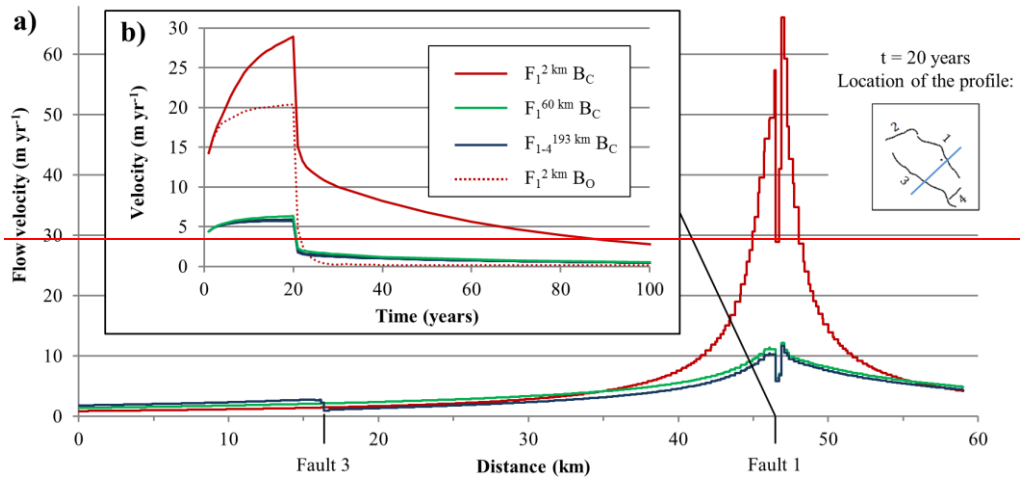

Figure 8. (a) Velocity profile within the lower element layer of the Rupelian basal sands shows highest flow velocities out of Fault 1 at the end of injection period. (b) Flow velocities out of Fault 1 increase until the end of the injection period (20 years) and decrease afterwards depending on pressure reduction of the respective scenarios.

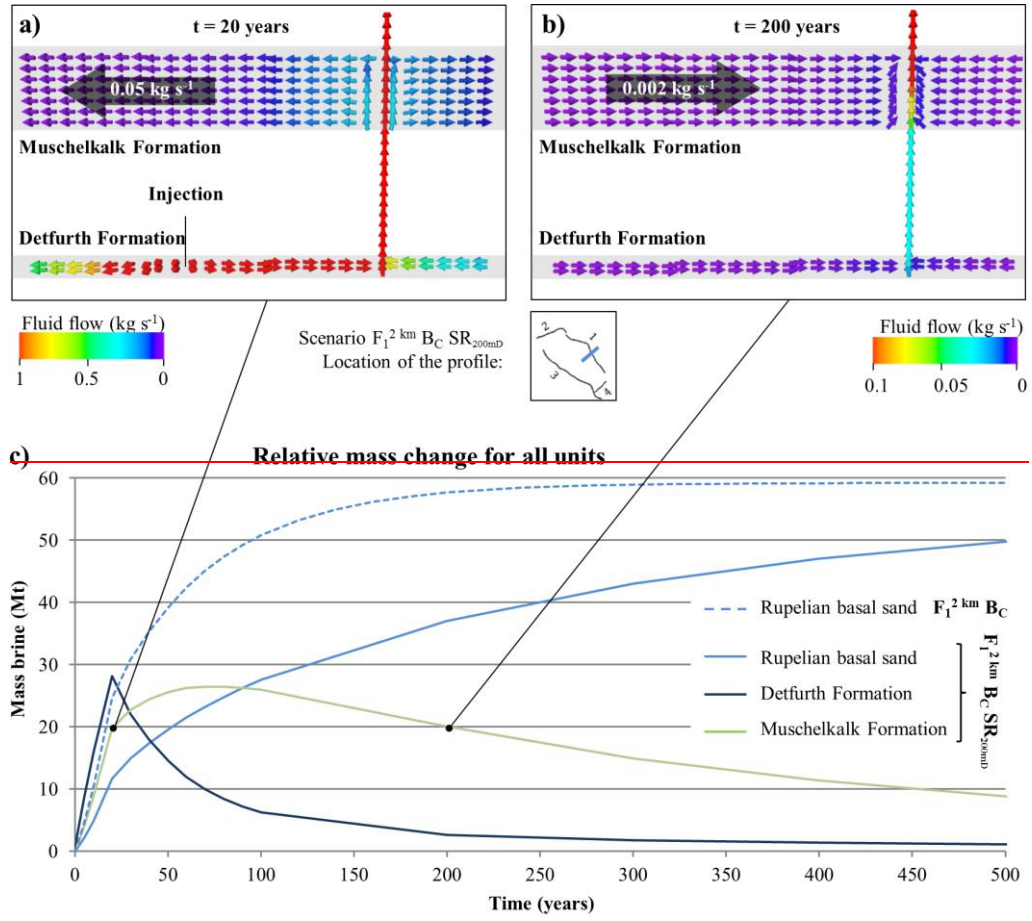

~~Figure 9. (a) Cross-profile normal to Fault 1 shows, that during the injection period the displaced fluid spreads within the Detfurth and the Muschelkalk. (b) Afterwards, brine is transported out of the respective reservoir due to pressure reduction in both reservoirs. (c) Temporal evolution of the relative mass change shows the resulting retardation in fluid flow into the Rupelian basal sands for scenario F_1^{2km} B_C SR_{200mD}.~~

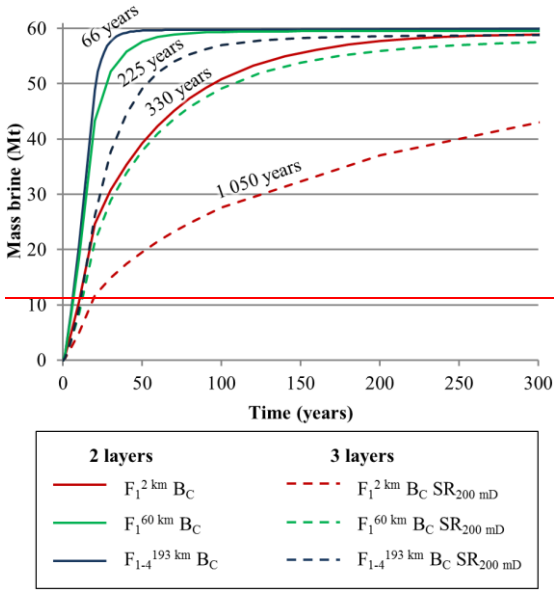

~~Figure 10. Relative mass change of the Rupelian basal sands illustrates the retardation in fluid flow (black numbers) due to the existence of an overlying reservoir, while the overall displaced brine mass into the shallow aquifer is almost identical, when pressure comes to equilibrium.~~

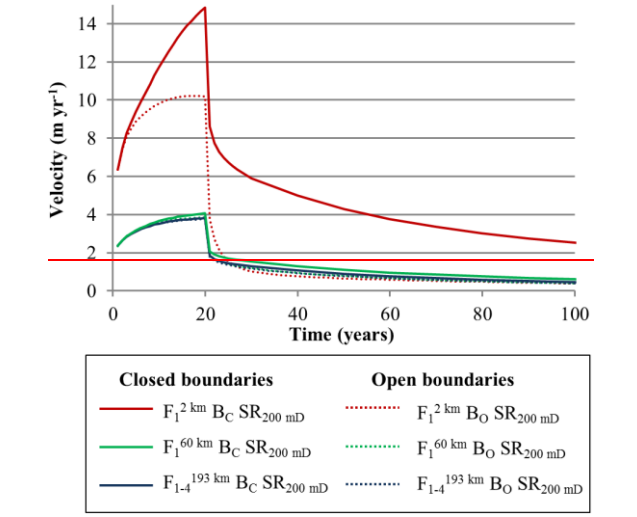

~~Figure 11~~

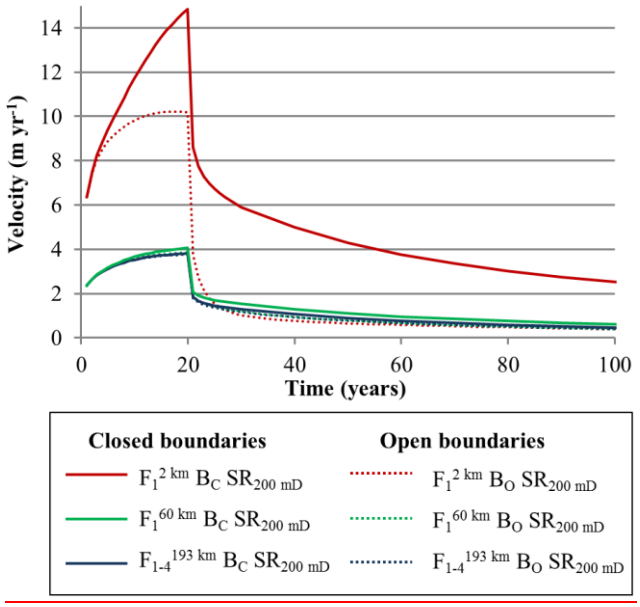

Figure 8. The temporal evolution of the flow velocities out of Fault 1 show a substantial reduction due to lower reservoir pressures for the scenarios considering a secondary overlying reservoir as well as open boundaries.

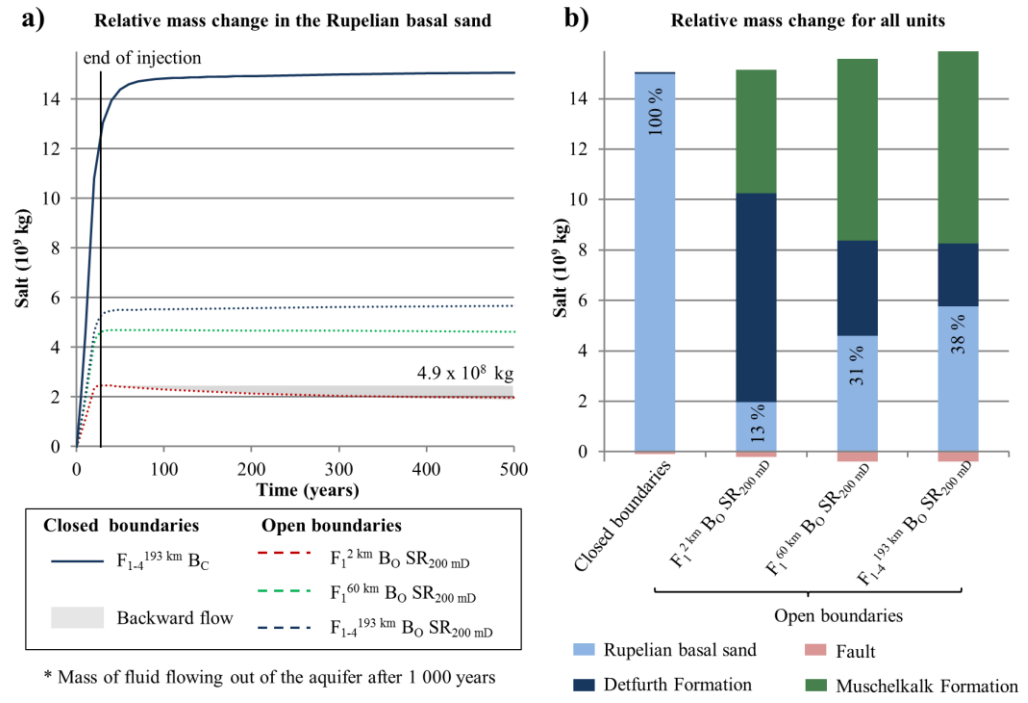

* Mass of fluid flowing out of the aquifer after 1 000 years

Figure 9.

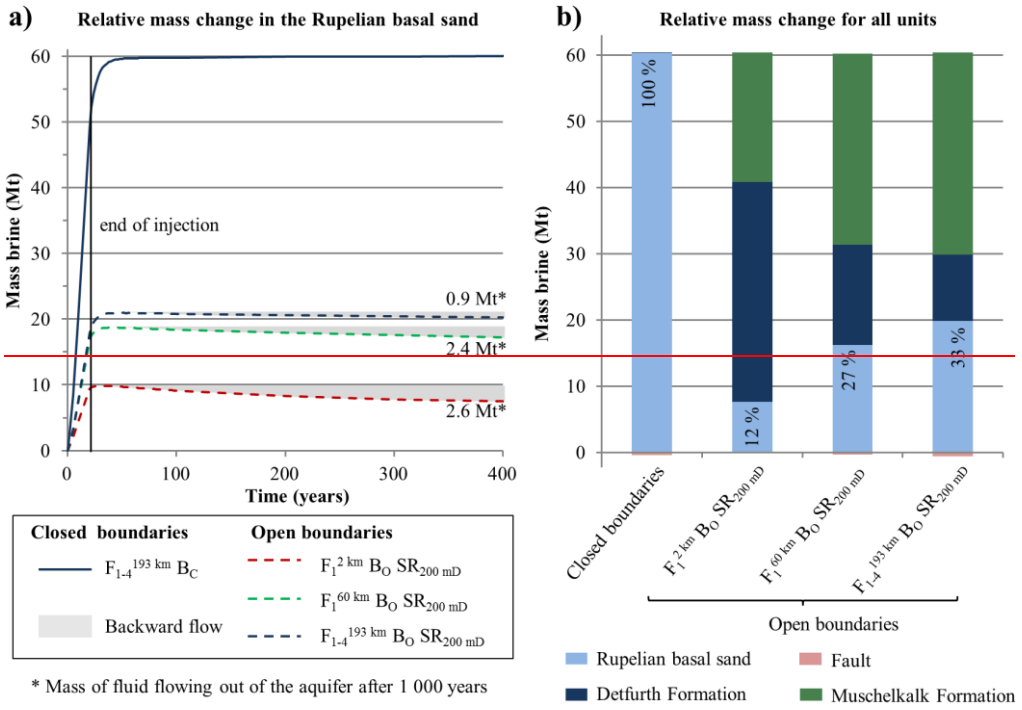

* Mass of fluid flowing out of the aquifer after 1 000 years

~~Figure 12.~~ (a) Temporal evolution of the relative mass change of the Rupelian basal ~~sands~~sand shows a lower duration of mass flow for open reservoir boundary conditions. Further, a slight backward flow out of the aquifer can be observed if the hydraulically conductive fault length is small. (b) Relative mass change for lithological units at 1 000 years (considering the backflow) illustrates, that salinization in the shallow aquifer is substantially reduced, if reservoir boundaries are open, and further an overlying secondary reservoir exists.

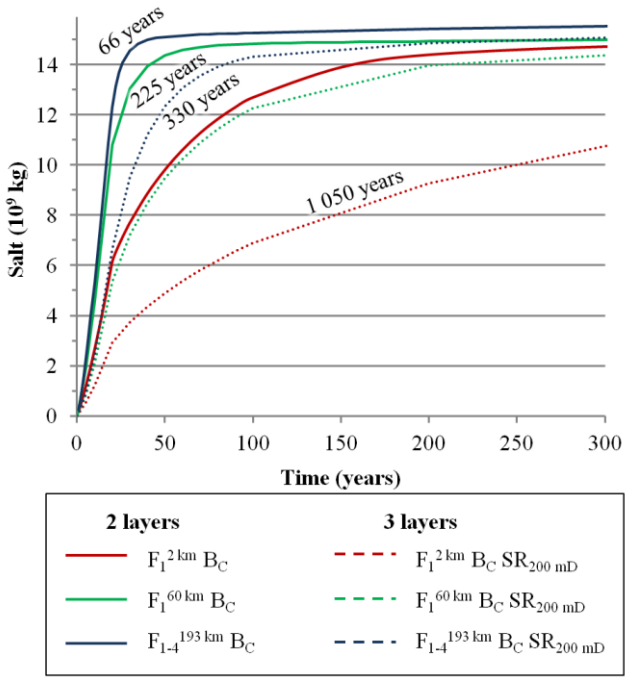

Figure 10. Relative salt mass change of the Rupelian basal sand illustrates the retardation in fluid flow (black numbers) in case of closed reservoir boundaries and due to the presence of an overlying reservoir. The salt mass that is displaced into the shallow aquifer is almost identical, when pressure comes to equilibrium.

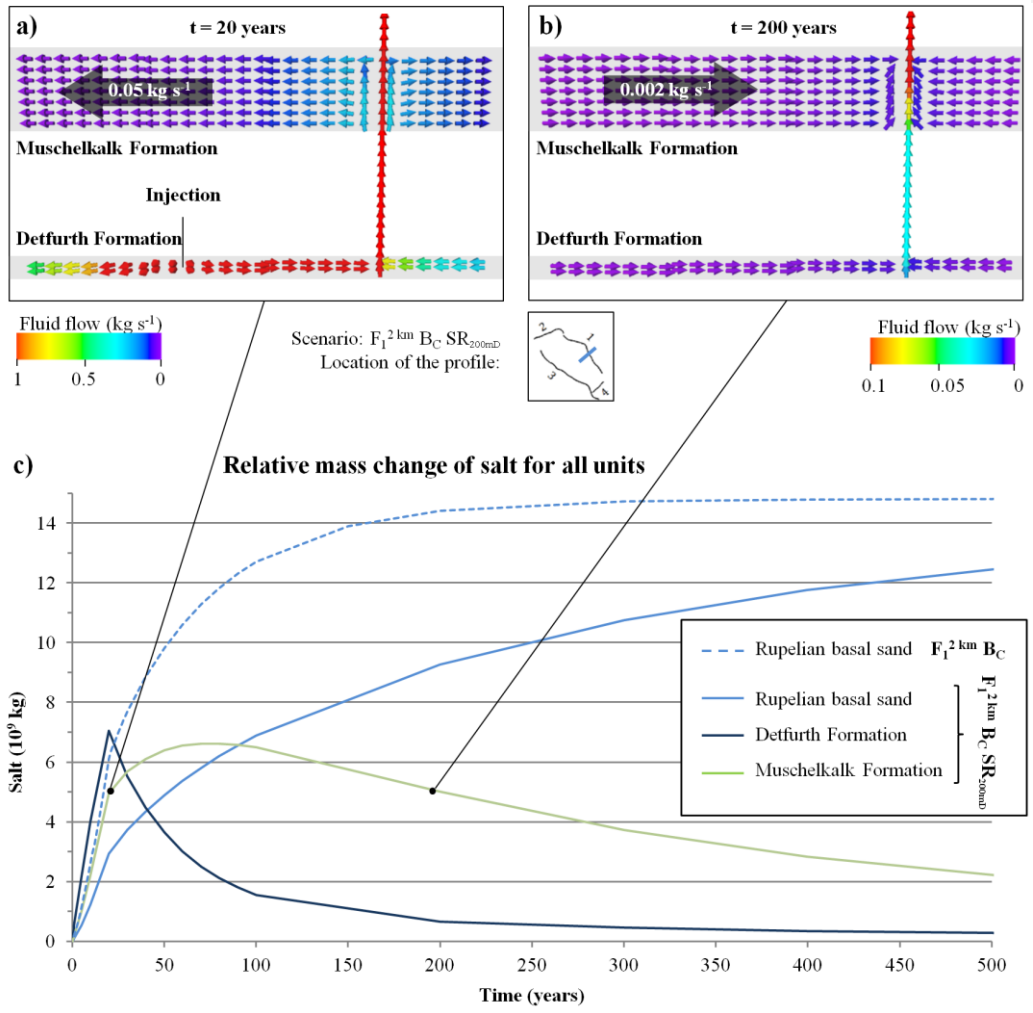
a)
t = 20 years
0.05 kg s-1
Muschelkalk Formation
Injection
Detfurth Formation
Fluid flow (kg s-1)
1
0.5
0
b)
t = 200 years
0.002 kg s-1
Muschelkalk Formation
Detfurth Formation
Fluid flow (kg s-1)
0.1
0.05
0
Scenario: F1 2 km BC SR200mD
Location of the profile:
c)
Relative mass change of salt for all units
Salt (10^9 kg)
Time (years)
Rupelian basal sand F1 2 km BC
Rupelian basal sand
Detfurth Formation
Muschelkalk Formation
F1 2 km BC SR200mD

1

Figure 11. (a) Cross profile normal to Fault 1 shows, that during the injection period the displaced fluid spreads within the Detfurth and the Muschelkalk.

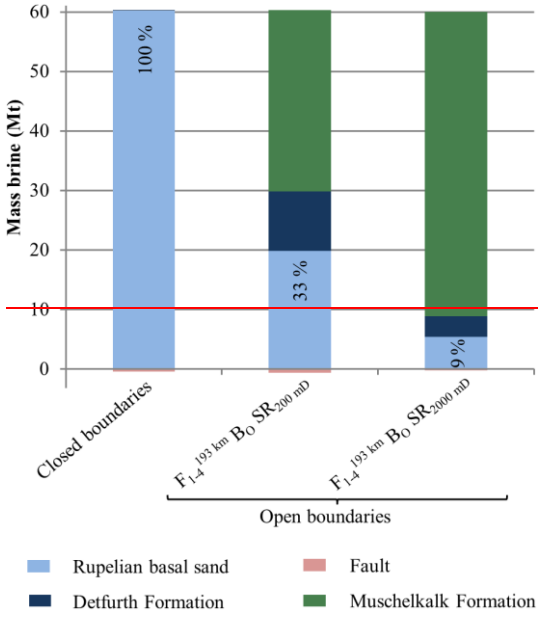

(b) Afterwards, the overpressure in both reservoirs is successively reduced and brine is transported out of the respective reservoir and into the Rupelian basal sand. (c) Temporal evolution of the relative salt mass change shows the resulting retardation in fluid flow into the Rupelian basal sand for Scenario F_1^{2km} B_C SR_{200mD}.

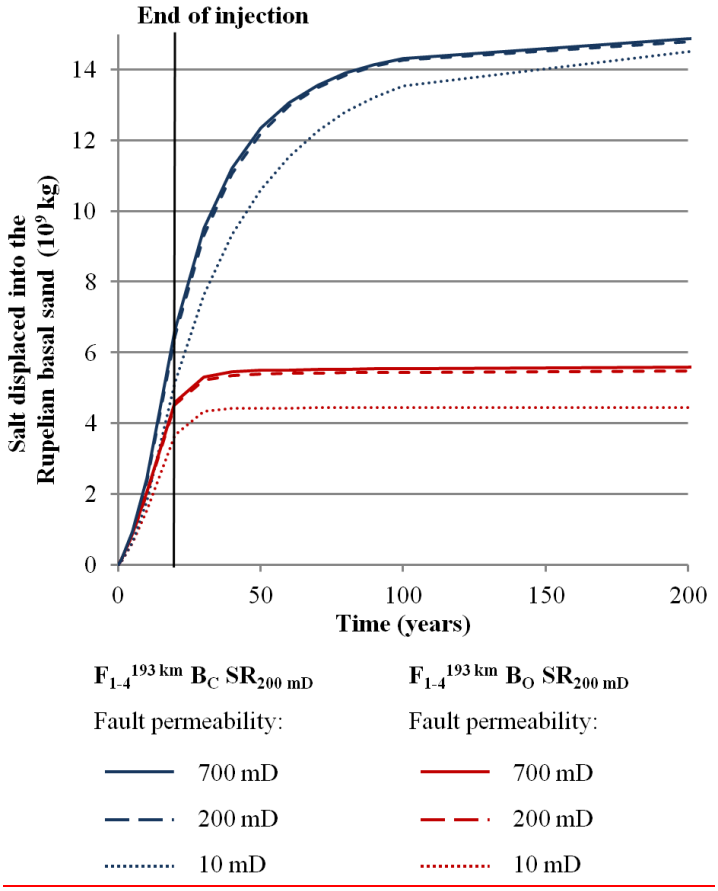

Figure 12. Salt mass displaced into the Rupelian basal sand assuming four open faults with varying permeability, a secondary overlying reservoir and open (red) or closed (blue) reservoir boundaries. The salt mass displaced into the Rupelian basal sand at the time of the injection stop and thereafter is almost identical for a fault permeability higher (solid lines) or equal (dashed lines) to the permeability of the secondary reservoir. If fault permeability is lower than that of the secondary reservoir (dotted lines), less salt is displaced into the shallow aquifer. Closed reservoir boundaries and low-permeable faults lead to retardation in mass flow (blue dotted line).

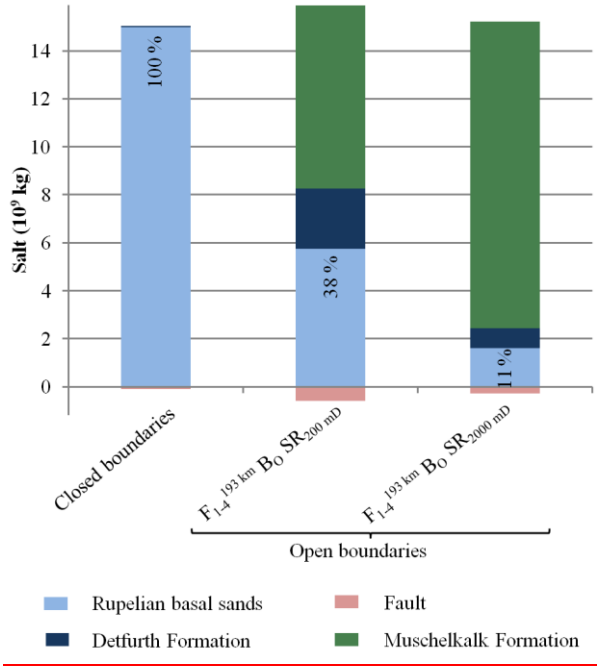

Figure 13. Relative mass change for all lithological units after 1 000 years ~~(considering the backflow)~~ illustrates that if permeability of the fault is lower than of the Muschelkalk Formation ($F_{1\text{-}4}^{193km}\,B_O\,SR_{2000mD}$) brine is preferentially displaced into the overlying secondary reservoir. Consequently, freshwater salinization in the shallow aquifer is lowest compared to all other scenarios with a sharp salt-/freshwater interface.

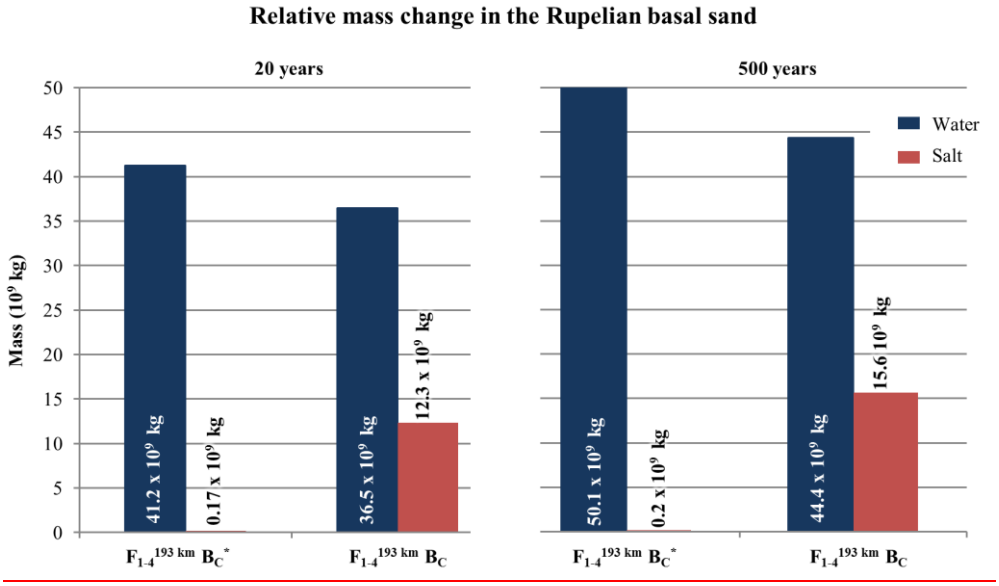

Figure 14. Relative mass change in the Rupelian basal sand after 20 years and 500 years for Scenario $F_{1\text{-}4}{}^{193km}\ B_C$ with a sharp salt-/freshwater boundary below the base of the Rupelian and Scenario $F_{1\text{-}4}{}^{193km}\ B_C{}^*$ with salinity increasing with depth by 0.23 g kg^{-1} solution per meter up to a maximum of 250 g kg^{-1} at a depth of 1 070 m.